A HIGH GAIN MULTI-INPUT INTERLEAVED BIDIRECTIONAL CONVERTER(MI-IBC) FOR ENERGY STORAGE APPLICATIONS

A PROJECT REPORT

submitted by

MEENU R.
(Reg. No. TKM21EEII08)

to

the APJ Abdul Kalam Technological University
in partial fulfillment of the requirements for the award of the Degree

of

Master of Technology
in
Electrical and Electronics Engineering
with specialisation in
Industrial Instrumentation and Control

Department of Electrical And Electronics Engineering

TKM College of Engineering
Kollam - 691005

JUNE 2023

DECLARATION

I undersigned hereby declare that the project report entitled "**A High Gain Multi-Input Interleaved Bidirectional Converter (MI-IBC) for Energy Storage Applications**", submitted for partial fulfillment of the requirements for the award of degree of Master of Technology in Electrical and Electronics Engineering with specialisation in Industrial Instrumentation and Control, of the APJ Abdul Kalam Technological University, Kerala is a bonafide work done by me under the supervision of *Dr. Muhammed Shanir P P*, Project Supervisor, Assistant Professor, Department of Electrical and Electronics Engineering, *Prof. Amal A*, Project Co-ordinator, Assistant Professor, Department of Electrical and Electronics Engineering. This submission represents my ideas in my own words and where ideas or words of others have been included, I have adequately and accurately cited and referenced the original sources. I also declare that I have adhered to ethics of academic honesty and integrity and have not misrepresented or fabricated any data or idea or fact or source in my submission. I understand that any violation of the above will be a cause for disciplinary action by the institute and/or the University and can also evoke penal action from the sources which have thus not been properly cited or from whom proper permission has not been obtained. This report has not been previously formed the basis for the award of any degree, diploma or similar title of any other University.

Kollam
June, 2023

MEENU R.

DEPARTMENT OF ELECTRICAL AND ELECTRONICS ENGINEERING

TKM COLLEGE OF ENGINEERING KOLLAM-691005

CERTIFICATE

This is to certify that the project report entitled "**A High Gain Multi-Input Interleaved Bidirectional Converter (MI-IBC) for Energy Storage Applications**" submitted by **MEENU R.** , **(Reg. No. TKM21EEII08)** of fourth semester to the APJ Abdul Kalam Technological University in partial fulfillment of the requirements for the award of the Degree of Master of Technology in Electrical and Electronics Engineering with specialisation in Industrial Instrumentation and Control, is a bonafide record of the project done by her under our guidance and supervision. This report in any form has not been submitted to any other University or Institute for any purpose.

Dr. Muhammed Shanir P P
Assistant Professor
Project Supervisor
Department of Electrical & Electronics Engg.
TKM College of Engineering Kollam

Prof. Amal A
Assistant Professor
Project co-ordinator
Department of Electrical & Electronics Engg.
TKM College of Engineering Kollam

Prof. Shanavas T N
Associate Professor and PG Co-ordinator
Department of Electrical & Engineering Engg.
TKM College of Engineering Kollam

Dr. Sabeena Beevi K
Associate Professor and Head
Department of Electrical & Electronics Engg.
TKM College of Engineering Kollam

ACKNOWLEDGMENT

A lot of effort and hard work has been put into this project in course of its presentation. However, it would not have been possible without the kind support help of many individuals and other sources. I take this opportunity to express my deep sense of gratitude and sincere thanks to all who helped me to complete this project report successfully. I thank God Almighty for paving my way throughout the project.

I express my special thanks to *Dr. T A Shahul Hameed*, principal of TKM College of Engineering for his timely support extended throughout the work.

I thank *Dr. Sabeena Beevi K*, Associate Professor and Head, Department of Electrical and Electronics Engineering, and *Dr. Imthias Ahamed T P*, Professor and Head Center for Artifical Intelligence and *Prof. Shanavas T. N*, Associate Professor and PG Co-ordinator, Department of Electrical and Electronics Engineering, *Prof. Amal A*, Project Co- ordinator, Assistant Professor, Department of Electrical and Electronics Engineering, for their support.

I am greatly thankful to my supervisor *Dr. Muhammed Shanir P P*, Assistant Professor, Department of Electrical and Electronics Engineering, for his supervision, assistance and helpful suggestions.

I wish to place my sincere thanks to *Mr. Lijin K L*, Research Scholar, Department of EEE, for his valuable suggestion, help and support for the successful completion of my work.

I wish to thank Prof. Sumayya Jaleel, Assistant Professor, Department of Electrical and Electronics Engineering, for her excellent guidance, positive criticism and valuable comments.

Finally I thank my parents and friends near and dear ones who directly and indirectly contributed to the successful completion of my project presentation.

MEENU R.

ABSTRACT

DC-DC converters are frequently used in electric vehicles, energy storage systems, and DC microgrids to convert a DC voltage from one level to another. Bidirectional DC-DC converters are converters that allow power to flow in both forward and backward directions. Bidirectional converter with high gain voltage is essential for energy conversion applications such as vehicles, medical devices, smart lighting's etc. This work proposes a high gain multi-input bidirectional DC-DC converter for the interface between an energy storage system and a DC micro-grid, which is important for DC-DC topologies. An Interleaved Bidirectional Converter (IBC) is located in the Low Volatge Side (LVS) to reduce the ripple in input current as well as output voltage. A voltage doubler is located in the High Voltage Side (HVS) to achieve high gain voltage conversion ratio. A simple and cost effective PWM plus Phase Shift (PPS) control is used in this work. As a modification to the existing bidirectional DC-DC converter for charging stations, PV panel is introduced as one of the input sources to create a cost-effective charging system, makes the proposed converter as a multi-input DC-DC converter. Zero-oscillation Maximum Power Point Tracking (MPPT) algorithm is used to extract maximum power from solar PV panels. Based on the available irradiation level, the control topology selects either a PV panel or a DC source as the input. To verify the effectiveness of the proposed converter and control topology, 800 W, 240V MI-IBC with switching frequency 30 KHz is designed and simulated in this work.

Contents

List of Tables

List of Figures

ABBREVIATIONS

DC	Direct Current
EV	Electric Vehicle
HVS	High Voltage Side
IBC	Interleaved Bidirectional Converter
LVS	Low Voltage Side
MI-IBC	Multi-Input -Interleaved Bidirectional Converter
MPP	Maximum Power Point
MPPT	Maximum Power Point Tracking
P&O	Perturb and Observe
PPS	PWM plus Phase Shift
PV	Photovoltaic

NOTATIONS

C	Capacitance
D_p	Duty cycle of LVS
D_s	Duty cycle of HVS
F_s	Switching Frequency
L	Inductance
P	Power
R	Resistance
V_1	Input voltage in LVS
V_2	Output Voltage in LVS
V_c	Capacitor Voltage in LVS

Chapter 1

INTRODUCTION

1.1 GENERAL BACKGROUND

Over the last few decades, more people have been using electric vehicles (EV). An EV is one that uses an electric motor instead of an internal combustion engine. Even though the conventional vehicles make transportation easier but they are affecting our health and the environment adversely. Conventional vehicles use fuel and emits greenhouse gasses like carbon dioxide, methane, nitrous oxide, and various synthetic chemicals and these emissions reduces the quality of air which led to the development of EV. EV have fewer moving parts than conventional vehicles, this creates less friction and makes no noise. Figure 1.1 shows the diagram of EV charging station.

Figure 1.1: EV charging station

Charging an EV involves the supply of DC power to the battery, here DC converters are used as an interface between energy storage device and DC microgrid bus. DC-DC converters are frequently used in electric vehicles, energy storage systems, and DC microgrids to convert a DC voltage from one level to another. When compared to the cost of refuelling a conventional Internal Combustion (IC) engine vehicle for the same distance travelled, the cost of charging

an Electric Vehicle (EV) with electricity is significantly less expensive. However, charging an EV from an AC grid uses more power in a shorter time. This results in voltage instability and phase unbalance on the distribution network, which has a negative impact on the operation of the distribution network and connected load. In order to solve these problems, charging stations powered by solar energy have been developed. Solar energy is renewable source of energy and does not emit greenhouse gasses or other harmful gasses contributing to air pollution. A solar electric vehicle is an electric vehicle powered by direct solar energy. The time taken to charge an EV depends on the amount of sunlight incident on the solar panels placed on the roof surfaces of electric vehicles. Solar panel capture the incident solar radiations and it is converted to electrical energy. DC-DC converters are used to boost the voltage from the solar panel and a storage battery is used to store the electricity generated from the solar panel. Solar panels are depends on the irradiation level, ambient temperature etc, so the use of solar energy is unreliable due to different climatic conditions. So a concept of multi-input source such as fixed DC and PV source is introduced in this work. A DC source and a PV source are integrated to develop a system, which is cost effective and reliable.

1.2 OBJECTIVES

- To design a high voltage gain bidirectional DC-DC converter with voltage doubler for energy storage application.
- To design a reliable and efficient energy source using multi-input DC-DC converter with solar PV panel and a fixed DC source as input voltage sources.
- To design a Pulsewidth Modulation plus Phase Shift control (PPS) for output voltage regulation.
- To compare and analyse different MPPT algorithms to get maximum power from solar PV panels.

1.3 SCOPE

A high-gain bidirectional DC-DC converter with a PPS control strategy is developed to regulate the desired value of the output voltage for the charging of EV. For cost-effective technology,

a PV source with zero oscillation MPPT algorithm is introduced as an input to the converter, which harvests the maximum amount of power from available solar energy. Due to the unreliability of solar radiation as a result of rapidly changing environmental conditions, the PV source has been integrated with a constant DC source that provides a constant output voltage for EV charging applications.

1.4 ORGANIZATION OF PROJECT WORK

The organisation of the report is as follows: Chapter 2 discusses various previous works related to different types of DC-DC converters used in EV charging stations. Different types of DC-DC converters, such as boost converters, interleaved bidirectional converters, and interleaved boost converters, are explained in Chapter 3. This chapter also includes a brief explanation of the voltage doubler required for the system and the block diagram of the system, DC-DC converter and PPS control topology. Chapter 4 gives a description of different MPPT methods such as P&O, multistep P&O, and the zero oscillation algorithm. The simulation model and results are depicted in Chapter 5, from which the results of the developed system are analysed. Conclusion from the previous chapters is explicated in chapter 6.

Chapter 2

LITERATURE REVIEW

2.1 OVERVIEW

The purpose of this project is to construct a high voltage gain multi-input interleaved bidirectional DC-DC converter with PPS control topology. The literature related to various bidirectional DC-DC converters, control topologies and maximum power point tracking (MPPT) techniques is discussed to develop the proposed system. The contributions of each paper are explained below.

2.2 BIDIRECTIONAL DC-DC CONVERTER

Bidirectional DC-DC converters (BDC) are very important and are used in many application, such as storage interface [1], [2] and Electric Vehicles [3]. Bidirectional dc–dc converters are needed for all energy conversion applications as they allow high voltage and low voltage to interact between each other[4]. Traditional BDC with two switches that are not isolated and not good for these applications because it needs very high duty ratios in boost mode and in buck mode . In [5] the voltage in the low-voltage side (LVS) and the voltage in the high-voltage side (HVS) are clamped by energy storage devices and DC microgrids, respectively. Most energy storage has low voltage ratings, and connecting storage cells in series makes them less reliable [6]. So a high gain of voltage conversion is necessary for DC-DC topologies. Out of the two types of converters, isolated and non-isolated converters, the voltage gain of non-isolated converter is limited by the duty cycle. Isolated BDC uses a transformer as the isolating element, which makes it possible to change the turns ratio and helps to reach high conversion

ratios. But in a full-bridge isolated BDC, there are usually at least eight active switches [7], [8]. Leakage inductance can cause voltage stress, so these topologies use clamped capacitor circuits [9] to avoid it. This makes it even harder to control these BDC. In [10], a new soft-switching DC-DC converter topology for high-power applications is studied. This converter has two three-phase inverter stages that operate in a high-frequency six-step mode, which reduces switching losses and accelerates switching frequency. High-frequency isolated DC-DC converters are recommended because their voltage conversion can be easily changed by changing the turns ratio of the transformer. Some isolated DC–DC Converters use a transformer to get a high-gain conversion, but the leakage inductance and parasitic capacitance cause high voltage or current spikes on the power devices.

Dual active bridge converters are the most popular isolated bidirectional converters due to their bidirectional power flow capacity, high power density, soft switching, and cascaded or paralleled modularity [11], [12]. In [13] focuses on the dual-active-bridge (DAB) DC-DC converters in power electronic traction transformers. Model-predictive control with current stress-optimized (MPC-CSO) based on dual-phase-shift (DPS) control is suggested to improve the dynamic performance, balance the transmission power, and get the current-stress optimization. The operation principles and switching modes of a dual H-bridge-based DC–DC converter were analysed in [14], and the expressions for voltage ripple and relation between voltage, current, and power are deduced. In the case of a Hybrid Dual-Active-Bridge DC-DC converter that is fed by a current [15]. It sets the duty cycle of the switches on the primary side to 0.5 to reduce the ripple in the input current and get high power conversion efficiency and a high gain in voltage. As it uses ten switches, it is expensive. So a new converter is introduced in [16] which presents a converter with ripple free input current for renewable energy systems. This converter can produce significant step-up voltage gain with a minimum number of devices and a low turns ratio transformer by using a switching operation on the secondary side. A secondary series-resonant circuit reduces switching losses and achieves high power conversion efficiency over the whole range of operation.

Some current-fed converters have been made to cut down the circulating current and increase the input voltage range. Some current fed converters are to boost the converter's efficiency under light loads, [17] suggested a Dual Phase Shift Modulation (DPSM) for an active commutated current-fed dual active bridge for low-voltage (LV) high-power applications. The phase shift between the legs on the HV side helped to lower the LV diode current, which in turn lowered

the circulating current in the converter. The two degrees of freedom in the proposed modulation helped to improve the performance of the converter by controlling the peak current based on the load. This is better than the simple PSM control, which only has one variable. This is done in the opposite direction to increase the ZVS range in the high voltage side. However the disadvantage is ZVS failure at the light load condition. In order to increase the ZVS and reduce the current ripple, an interleaved structure is designed. A traditional voltage-matching (VM) control is used for bidirectional converters to minimise the RMS of the inductor current [18]. The basic topology with interleaved structure is studied in [19]. Intermediate capacitor-based topology is studied [20] in modification of initial topology to increase voltage gain but lost parallel inductor structure, which is helpful in sharing current during buck mode. Quasi-resonant operation of same [21] BDC structure where coupled inductor is replaced by simple inductor is studied [22], which is further generalised to make the topology suitable for high power applications. But the basic structure of the circuit stays the same. The proposal [23] uses an interleaved structure with two extra inductors to share the current. Even though topology [23] is better than [24] in terms of gain, stress level, and efficiency, the circuit is harder to operate because it has more parallel inductors. The performance of Phase-shift (PS) and PWM plus phaseshift (PPS) control schemes is compared in [25]to explore their detailed difference and give a design guidance for the industrial applications. The comparison results show that the PPS control scheme is an optimal case of the PS control with some control complexity and have many advantages compared with the PS control strategy. The converter proposed in is designed to reduce current ripples that are fed into renewable energy resources. Many of the control strategies that have been suggested in past studies are complicated, so the phase shift ratios have to be calculated by math software [26]. To do computation in real time, an online control strategy is proposed [27]. It operates on a coupling relationship between its three variables, which include one duty cycle and two phase shift angles. Due to the complexity of most modulation schemes, a high-performance digital controller is essential for real-time operations [28]. Many research projects focus on comprehensive optimization schemes [29] [30] to separate multiple control variables and make a simple control strategy. This is done to reduce the amount of computing that needs to be done. In [31], a high voltage-gain bidirectional DC-DC converter is proposed using decoupling control. A voltage doubler is used in the high voltage side to double the voltage. Thus the overall conversion efficiency is high and reduces switching losses.

An electric vehicle charging station is a equipment that connects EVs to a source of electricity to recharge them. It is a lengthy charging process and it is unreliable due to the lack of available charging outlet port, much research has been done to use renewable energy resources as the input to the system. When solar PV panels are added, the input of the converter becomes unstable because the voltage and power of the solar PV panels change depending on the temperature and irradiance. Different Maximum Power Point Tracking (MPPT) methods [32], [33], [34], [35], [36], [37] are used to get the maximum energy out of solar PV panels in different climatic conditions. There are two type of charging station: ON grid and OFF grid solar charging station. ON grid solar charging station charges the EV by using power grid to transfer electricity from an off grid source i.e, solar energy to EV. Off grid solar charging station uses direct current to power electric EV's. In [38] proposes a electric vehicle charging station suitable for multiple electric vehicles. This electric vehicle charging station model was designed to support vehicle to grid and reactive power compensation. [39] modeled an EV charging station for DC quick charging of multiple EV simultaneously. General faults that occur commonly in a charging station is implemented to the modeled EV in [39] and studied the effects of fault and implemented a protection scheme that would eliminate the faults. In [40] discusses a two input single output DC-DC converter for EV charging with solar source as one of the input. The overall efficiency of the system increases by the integration of PV source with DC source. This work is concentrated on DC-DC converter in EV charging with Fixed DC, PV source in three modes such as fixed DC only, PV source only and PV integrated with DC source.

2.3 SUMMARY

This chapter discusses previous work related to this research domain. This review focuses on different types of BDC converters, its operation, applications and disadvantages and which leads the decision of using interleaving technology in bidirectional DC-DC converter to reduce the ripple percentage. Previous publications related to various MPPT control algorithms for harvesting maximum power from solar PV and work related to EV charging stations is also included here. Different DC-DC converter topologies and proposed system is explained in the next chapter.

Chapter 3

HIGH VOLTAGE GAIN BIDIRECTIONAL DC-DC CONVERTER

3.1 OVERVIEW

Based on studies and a review of the literature, it has been found that the interleaving technology in bidirectional DC-DC converters can reduce the amount of output voltage and current ripple. The pps control topology is introduced to reduces the control complexity of the system. This chapter covers different DC-DC converters such as boost converters, interleaved bidirectional converters, and interleaved boost converters and their working. This chapter gives a brief explanation of the voltage doubler circuit and how it works in this proposed system. For better understanding, the block diagram of the system, the DC-DC converter, and the control topologies are explained.

3.2 DC-DC CONVERTER

A DC-DC converter is an electrical circuit which converts DC voltage from one voltage level to another. They are widely used in regulated switch mode DC power supplies and in DC motor drive applications. There are two types of DC-DC converter linear and switched mode DC-DC converter. Linear converters are the one which uses a resistive voltage drop to create and regulate the given output voltage. Switch mode DC-DC converters stores energy to the inductor periodically and releasing the stored energy to the output of different voltages. The energy is stored either in an inductor, a transformer or a capacitor.

DC-DC converter allows the power to flow only in one direction. A bidirectional DC-DC converter is used in the DC-DC conversion process because it enables power to flow in both directions. Typically used in energy storage in battery banks, renewable energy systems and so on.

On the basis of the isolation of load from the source the DC-DC converters are classified as :

- Isolated DC-DC Converters
- Non isolated DC-DC Converter

An isolated converter separates the input from the output, preventing direct current flow between the input and output, which is typically accomplished with the use of a transformer. The presence of the transformer in the isolated converter offers isolation between the input voltage and the output voltage, which eliminates the risks associated with electric shocks. However, the introduction of the transformer results in an increase in the converter's size, cost and weight. A non-isolated converter has a single circuit through which current can flow from input to output. This type of converter circuit uses switches, an inductor and a capacitor to transfer energy from the input to the output. Non-isolated converters are classified mainly into three types: buck, boost, and buck-boost converters. In a buck (step-down) converter, the output voltage produced is less than the input voltage. In a boost (step-up) converter, the output voltage is greater than the input voltage. The buck boost converter allows the input DC voltage to be either stepped up or stepped down, depending on the duty cycle.

Here are some advantages of using a bidirectional DC-DC converter in the battery charger of an electric vehicle:

- High effectiveness.
- Smaller in size and less bulky.
- EMI reduction (electromagnetic interference).
- Reduce the ripple in the input and output currents There are two kinds.
- Instead of varying the input voltage, power flow was controlled.

3.2.1 BOOST CONVERTER

A boost converter (step-up converter) is a DC-DC converter that increases the voltage from input to output. The working principle of the boost converter is the ability of the inductor to resist current either by increasing or decreasing the energy stored in the inductor magnetic field. Filters made of capacitors are typically added to the output and input of such a converter to reduce voltage ripple. The circuit diagram of boost converter is shown in Figure 3.1. The components in a boost converter circuit are an inductor, a capacitor and a switch. It has two modes of operation.

- Mode 1: When the switch is turned ON, the diode is reverse biased. The current will flows through the inductor, switch and back to DC source. The inductor stores energy and the polarity on the left side of the inductor is positive.

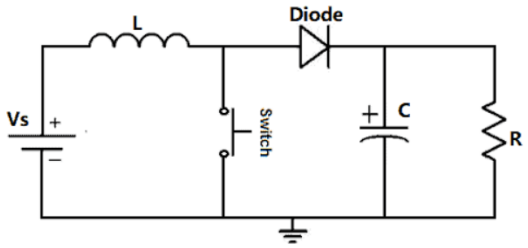

Figure 3.1: Circuit diagram of Boost Converter

- Mode 2: When the switch is turned OFF, the diode is forward biased. The polarity of the inductor is reversed and the energy stored in the inductor is released to the load. This helps to keep the flow of current in the same direction and also boosts the output voltage.

The waveform of inductor current in boost converter is shown in figure 3.2. The inductor charges during T_{on} and dischages during T_{off}. During T_{on} the switch is ON, the diode is reverse biased and this time the load is being supplied by the energy stored in the capacitor. The current flows from V_{in} to inductor L and switch S and the inductor will charge. Applying Kirchhoff's Voltage Law (KVL), the inductor voltage V_L is given by the equation 3.1

$$V_L = V_{in} - V_s \tag{3.1}$$

V_{in} is the input voltage and V_s is the turn on voltage of the switch. The voltage across the inductor is

$$V_L = L \times \frac{di}{dt} \tag{3.2}$$

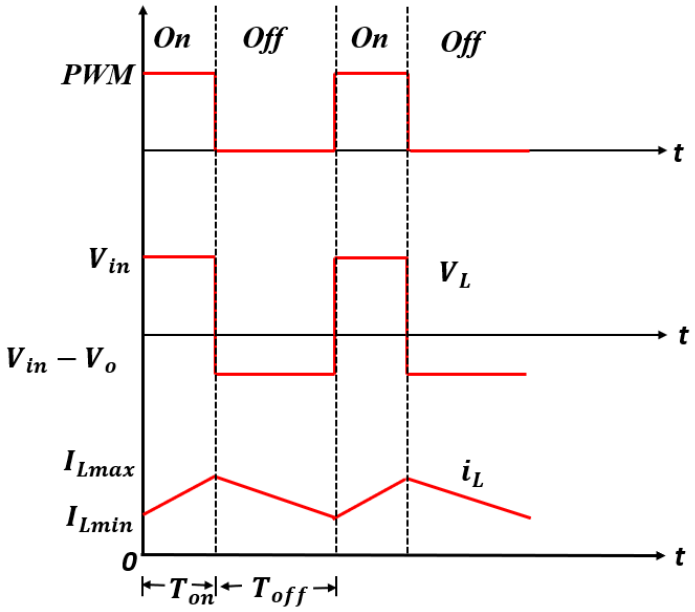

Figure 3.2: Waveform of inductor current in Boost Converter

Expressing the change in current di

$$di = \frac{V_L}{L} \times dt \tag{3.3}$$

substituting equation 3.1 in equation 3.3

$$di = \frac{V_{in} - V_s}{L} \times dt \tag{3.4}$$

Integrating the equation 3.4 from 0 to T_{on}

$$i = \int_0^{T_{on}} \frac{V_{in} - V_s}{L} \times dt \tag{3.5}$$

During T_{off} the switch is OFF, the diode is forward biased and at this time the load is being supplied by the energy stored in the inductor. The inductor will starts to discharge and current flows from V_{in} to diode D then to the load. Applying KVL

$$V_L = V_o + V_f - V_{in} \tag{3.6}$$

Substituting equation 3.6 in equation 3.3 results in

$$di = \frac{V_o + V_f - V_{in}}{L} \times dt \tag{3.7}$$

Integrating equation 3.7 from T_{on} to T

$$i = \int_{T_{on}}^{T} \frac{V_o + V_f - V_{in}}{L} \times dt \tag{3.8}$$

Equating equation 3.5 and eqaution 3.8

$$\int_0^{T_{on}} \frac{V_{in} - V_s}{L} \times dt = \int_{T_{on}}^{T} \frac{V_o + V_f - V_{in}}{L} \times dt$$
$$\mathrm{T_{on}}(V_{in} - V_s) = (T - T_{on})(V_o + V_f - V_{in}) \tag{3.9}$$

Substitute T_{on} = DT

$$DTV_{in} - DTV_s = T(1 - D)(V_o + V_f - V_{in}) \tag{3.10}$$

Then solving for the duty cycle D

$$D = \frac{V_o + V_f - V_{in}}{V_o + V_f - V_s} \tag{3.11}$$

Assuming diode and switch voltages as zero then the equation for duty cycle D is

$$D = \frac{V_o - V_{in}}{V_o} \tag{3.12}$$

Final equation for duty cycle is given by the equation 3.13.

$$D = 1 - \frac{V_{in}}{V_o} \tag{3.13}$$

Boost converters are advantageous because they provide a high output voltage compared to the input voltage, have low operating duty cycles, and have a lower voltage stress. Boost converters are used in power amplifier, battery power systems, Electronics and communication applications etc.

3.2.2 INTERLEAVED BOOST CONVERTER

Voltage and current ripples are produced in DC converters causes many undesirable effects in DC circuits, such as noise distortion, improper operation of the circuit, and the possibility of heating components etc. In order to overcome this ripple, a new topology is introduced, which is called interleaving. Interleaving is a technique in power converter design for switching multiple converter stages in parallel thus reducing the input current and output voltage ripples.

The phase difference between the gating pulses of the switches in interleaved converter is 360/n, where n is the number of parallel boost converters. Here the Converter (IBC) is made up of two boost converters connected in parallel with a 180° phase delay and running at desired frequency. The interleaved boost converter is better than a boost converter because it is more efficient, and reliable.

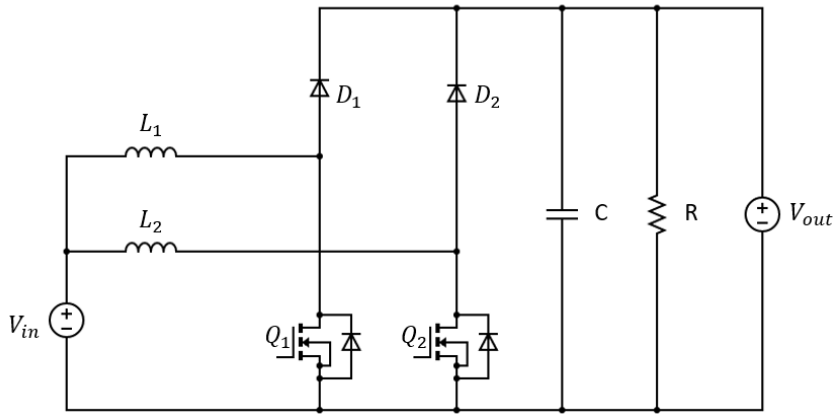

Figure 3.3: Circuit diagram of Interleaved Boost Converter

The schematic diagram of a two phase interleaved boost converter is shown in Figure 3.3. It consist of a combination of inductor, diode and switches in parallel. Switches Q_1 and Q_2 are triggered with switching pulses which enables the interleaving operation.

Mode1 : When the switches Q_1 and Q_2 are turned ON, the current flowing through the inductors L_1 and L_2 increases linearly. During this time, the capacitor provides energy to the load.

Mode2 : Q_1 is OFF and Q_2 is ON condition. Thus results in linear increase in current through L_2. The energy stored in the inductor L_1 forward biases the diode D_1 which allows the flow of input current to flow to the output stage through $Q_1$and D_1. The energy in the inductor L_1 is passed to the capacitor and the load.

Mode3:This is similar to the case when Q_1 and Q_2 are triggered.

Mode4: Next stage Q_2 is OFF and Q_1 is ON results in linear lincrease in current through the inductor L_1. The energy stored in the inductor L_2 forward biases the diode D_4 and the energy stored in the inductor L_2 is passed to the capacitor C_{boost} and the load. During this mode of operation the voltage is stepped up.

The diodes D_1 and D_2 in the interleaved boost converters are replaced by controlled switches Q_3 and Q_4 for the interleaved bidirectional operation of DC-DC converters which is shown in Figure 3.4. It consist of two modes of operation. One is boost and another is buck mode of operation. Switching is used to make this device to work in the boost and buck modes respectively.

Boost mode of operation: During boost mode of operation when the switch Q_1 and Q_2 are triggered the current flows through the inductor L_1 and L_2 increases linearly. During this

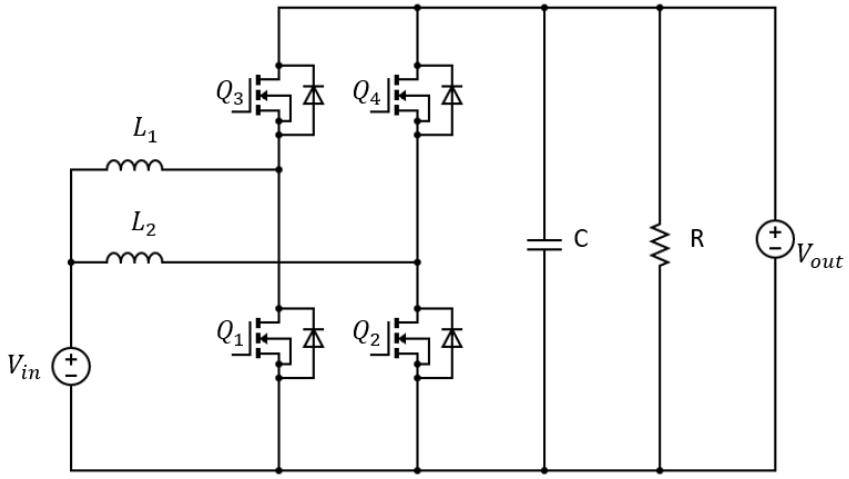

Figure 3.4: Circuit diagram of Interleaved Bidirectional Converter

period capacitor provide energy to the load. During this mode input voltage of the converter is boosted.

Buck mode of operation: During the buck mode of operation switches Q_3 and Q_4 are operated. When the switches are turned ON the current increases linearly. When the switches are turned OFF the energy stored in the inductor is transmitted to the load. During this mode input voltage of the converter is stepped down to 60V. For this work, only boost mode is considered. The bidirectional case is more difficult as the circuit becomes more complicated.

3.3 VOLTAGE DOUBLER

Voltage multiplier is an electrtonic circuit which multiplies or rises the voltage level. Voltage multiplier circuits are divided into three main types based on how they multiply voltage: voltage doubler, voltage tripler, and voltage quadrupler. A voltage doubler doubles the peak value of input voltage, a voltage tripler triples the peak value input of voltage, and a voltage quadrupler increases the voltage by four times the peak value of the input voltage. This work is concentrated on voltage doubler circuit. A voltage doubler is an electronic circuit that charges capacitors from the input voltage and switches these charged capacitors in such a way that exactly twice the voltage is produced at the output.

The circuit diagram of voltage doubler is shown in Figure 3.5. During the positive half cycle of the input AC signal, diode D_1 is forward biased. So the diode allows electric current to pass through it. This current will flows to the capacitor C_1 and charges it to the peak value of input

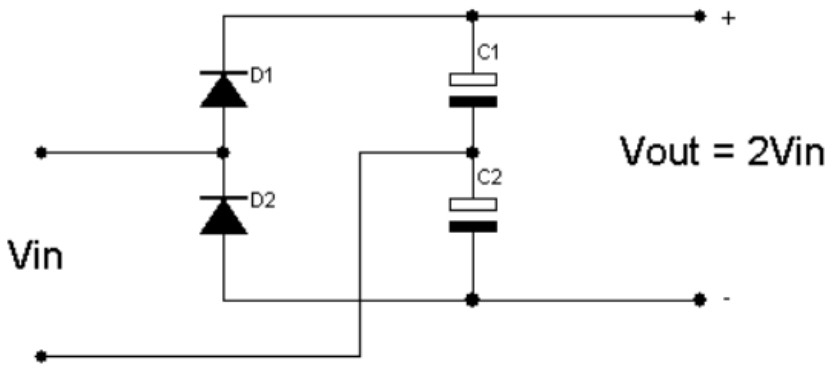

Figure 3.5: Circuit diagram of Voltage doubler

voltage V_{in}. Diode D_2 is reverse biased during the positive half cycle. So diode D_2 does not allow electric current through it, therefore capacitor C_2 is uncharged. During the negative half cycle of the input AC signal the diode D_2 is forward biased. So the diode D_2 allows electric current through it. This current will flows to the capacitor C_2 and charges it to the peak value of input voltage V_{in}. Diode D_1 is reverse biased during negative half cycle. So D_1 does not allow electric current through it.

The capacitor C_1 and C_2 are charged during alternate half cycle. If no load is connected to the output terminals, the output voltage V_o is equal to the sum of the capacitor voltages V_{C_1} and V_{C_2} ie

$$\begin{aligned} V_0 &= V_{c_1} + V_{c_2} \\ &= V_{\text{in}} + V_{\text{in}} \\ &= 2V_{\text{in}} \end{aligned} \tag{3.14}$$

When a load is connected to the output terminals, the output voltage V_o will be a little bit less than $2V_{in}$ The use of high voltage transformer is eliminated as the voltage changes from low voltage to high voltage at low rate. Negative voltage can also be produced by reversing the direction of the diodes and capacitors. By cascading similar voltage multipliers together, the voltage multiplier factor is raised. Voltage doublers are widely used in cathode ray tubes, in x-ray and radar systems along with LCD backlight, in laser systems and in oscilloscopes etc.

3.4 BLOCK DIAGRAM OF THE PROPOSED SYSTEM

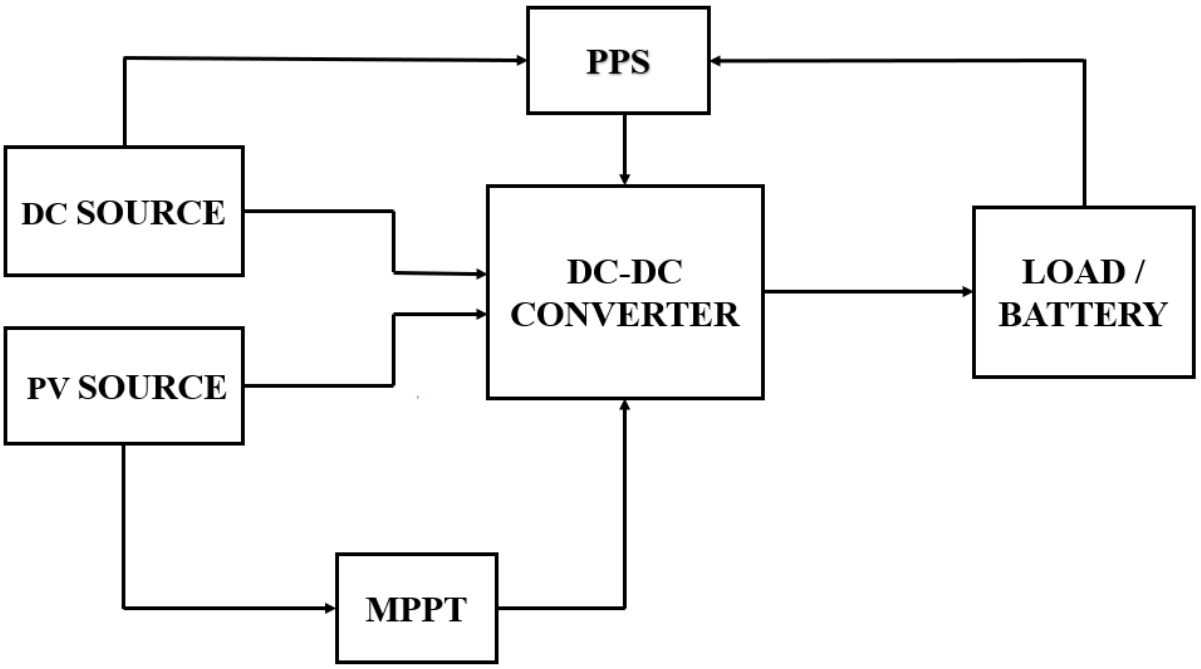

Figure 3.6: Block diagram of the proposed system

The block diagram of the proposed system is shown in figure 3.6. It consist of a fixed DC source, PV source, DC-DC converter, PPS control, MPPT control and a load/battery. DC-DC converter include interleaving (LVS) and voltage doubling (HVS) technology. PPS control is applied to both LVS and HVS of DC-DC converter when a DC source is used as the input to the proposed system. When solar PV panel is used as the input voltage source of the proposed system MPPT control is used in LVS and PPS control is used in the HVS of DC-DC converter.

3.4.1 BLOCK DIAGRAM OF DC-DC CONVERTER

The block diagram of the DC-DC converter in the proposed system is shown in Figure 3.7. This block diagram consist of Interleaved Bidirectional converter (IBC) , Voltage doubler, PV/Fixed DC source, PPS control, MPPT control and battery/load. DC source with input of 60V is applied to IBC converter. An isolation transformer is used to isolate the LVS and HVS side. An isolation transformer is a stationary device that physically and electrically separates the primary and secondary windings of the system. It sends electricity from one circuit to another by using a magnetic induction mechanism that uses a magnetic field to create EMF in another

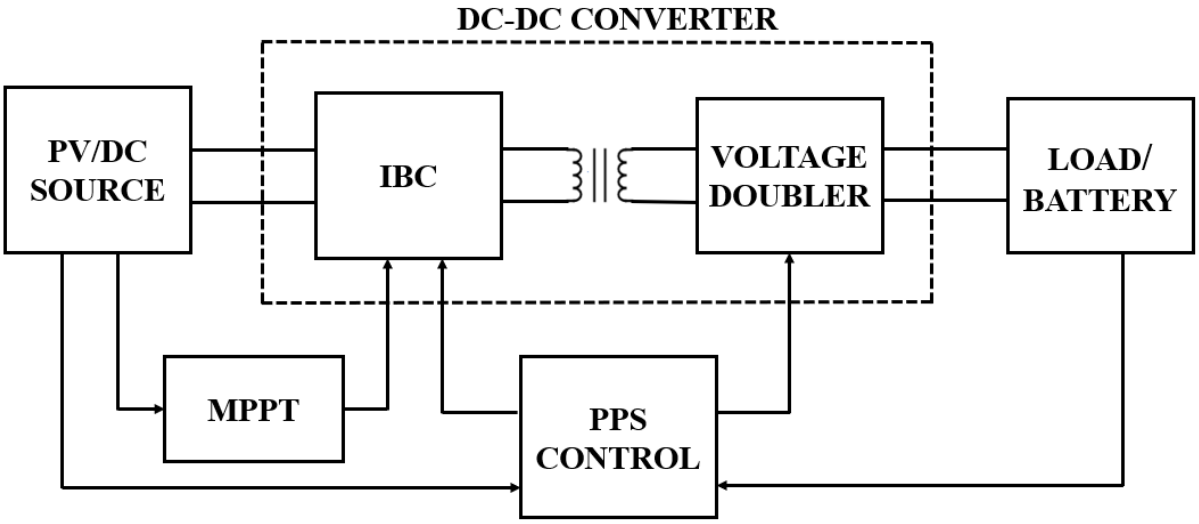

Figure 3.7: Block diagram of DC-DC converter

circuit without changing the frequency. Isolation transformer is used to protect the device from electric shocks or to transfer power between two devices.

3.4.2 BLOCK DIAGRAM OF PWM PLUS PHASE SHIFT CONTROL

The block diagram of the PPS control topology is shown in Figure 3.8. It consist of two control parts: voltage match control and power flow control. V_1 and V_2 are the voltages of the LVS and HVS respectively. I_2 is the current from HVS and P_{ref} is the reference power. Voltage match control part can be implemented by D_p derived from V_1 and V_2. The power flow control part can be implemented by the adjustment of phase angle using a PI controller.

The power from the HVS is compared with the reference power, and the difference is given to the PI controller. The output of the PI controller is the phase angle φ, which is given to the PWM to generate the driving signal. The change in duty cycle is represented by δD, which is selected as 0.002. Other two input to the PWM is D_p and D_s. In proposed control the control variables D_p and φ are separatly controlled. These driving signals are given to the switches of HVS and LVS when the system operates with DC source. While using MPPT these signals are used in HVS only.

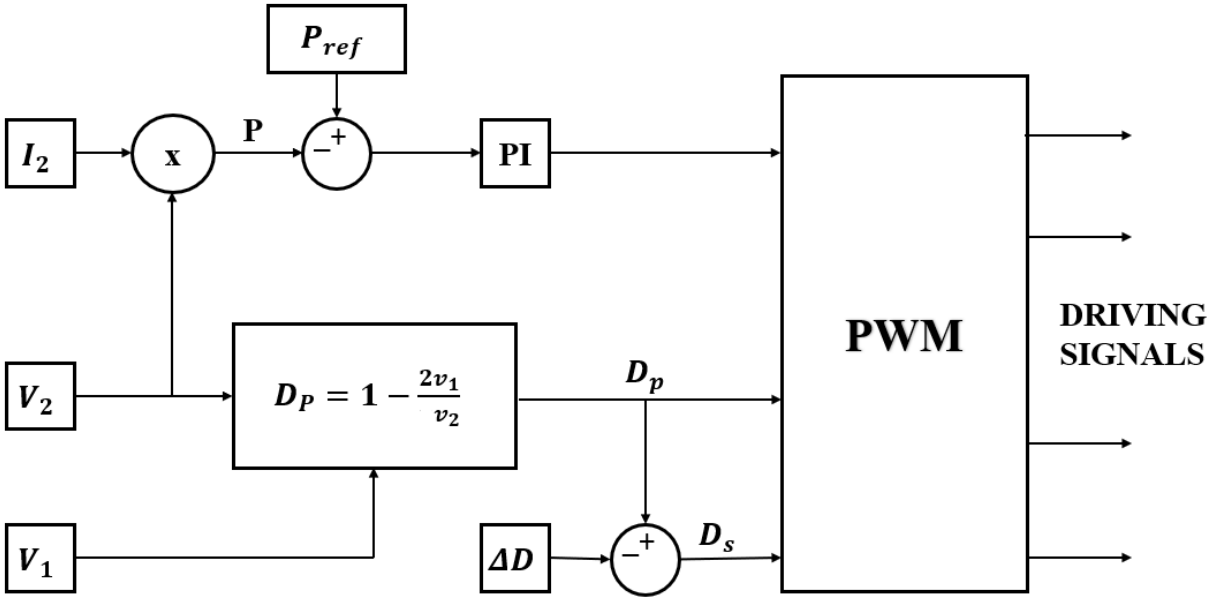

Figure 3.8: Block diagram of PPS control

3.5 SUMMARY

Different type DC-DC converters such as boost, interleaved boost and interleaved bidirectional converters and their workings are studied. The interleaved boost converters are advantageous over conventional boost converters, therefore this work focuses on interleaved boost converter on the LVS. The working logic of the voltage doubler circuit is depicted as it is a part of the system. The block diagram of the system, DC-DC converters and PPS control are provided to get a brief idea of the whole system. Next chapter discusses about the MPPT algorithms which includes P&O, multistep P&O and zero oscillation algorithm.

Chapter 4

MAXIMUM POWER POINT TRACKING

4.1 OVERVIEW

A sustainable way to charge an electric vehicle is to use electricity from renewable source of energy such as the sun, the wind, etc. In this work, solar energy is chosen as the renewable energy source, and a PV panel is used to absorb the radiation from the sun. Different MPPT algorithms such as PO, multistep PO, and zero oscillation are used to extract maximum power from the PV panel and comparison of aforementioned MPPT is done to determine the best among them.

4.2 INTRODUCTION

Maximum Power Point (MPPT), which stands for "Maximum Power Point Tracking," is an algorithm used to get the maximum power out of a PV module under certain conditions. The voltage at which the MPPT can produce maximum power is called Maximum Power Point (MPP). Maximum power varies with solar radiation, ambient temperature and solar cell temperature. Only 30 to 40 percent of the solar energy that hits a standard solar panel is turned into electricity. Maximum power point tracking is used to make the solar panel work better. There are different MPPT methods and designs. Each methods have its own specifications,limitations and applications. MPPT methods are classified based on different norms such as tracking technique, sensing implementation and contemporary. For each classification there are several subcategories

based on different factors, working principle or implementation. Based on tracking mechanism MPPT methods can be classified as: conventional, soft computing and hybrid methods. In this work P&O, multi-step P&O and zero oscillation methods are used which comes under conventional method.

4.2.1 PERTURB AND OBSERVE MPPT ALGORITHM

This is a conventional MPPT method which includes the perturbation in the voltage and maximum power output is measured. Figure 4.1 shows the flow chart of P and O algorithm. The fundamental principle of the P&O method is that the voltage is purposely perturbed to increase or decrease, and then the power is compared to what was acquired before the disruption. The power is raised if the preceding state's perturbation was positive, the power rise continued in that direction. When the prior state was perturbed positively , the power reduced and the current should be in the opposite direction. The power is increased when the preceding state's perturbation was negative and the perturbation is then continued in the same direction. The power is reduced, if the prior state had a negative perturbation, the current perturbation should go in the opposite direction.

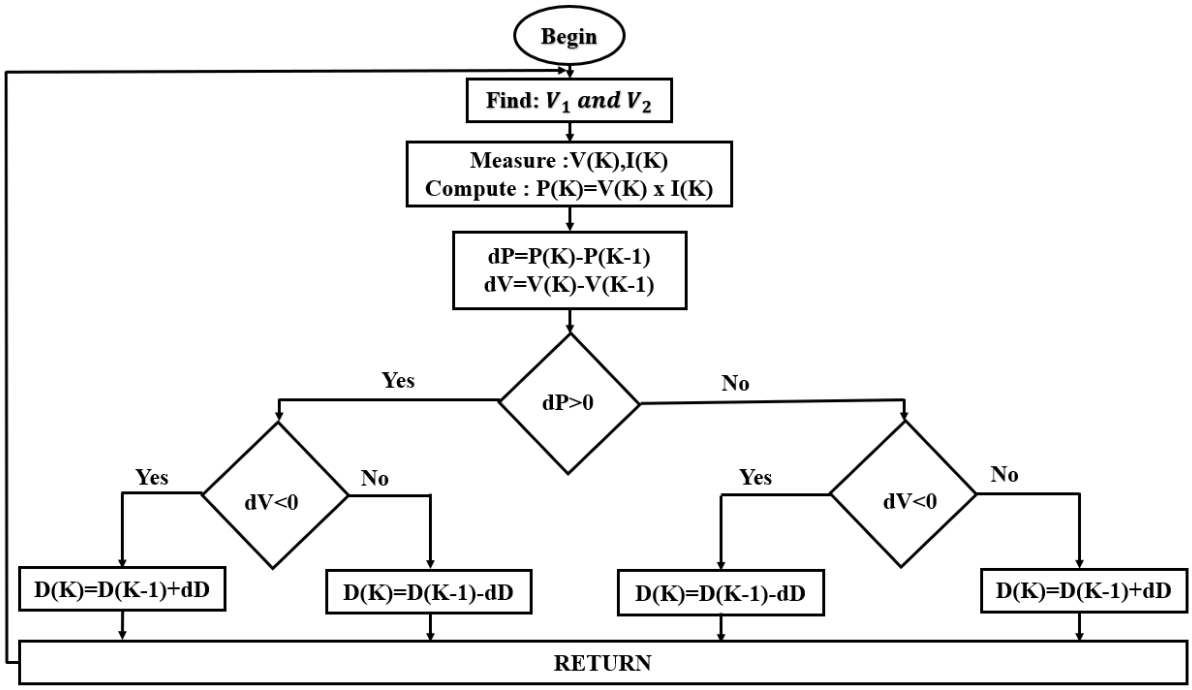

Figure 4.1: Flow chart of P&O algorithm

The main advantage of this method is that it doesn't have to figure out the complicated mathematical relationship between power output, solar irradiance, solar temperature, and total resistance. This algorithm is not appropriate for fast varying atmospheric conditions due to slow tracking. To overcome the limitations of P&O algorithm multistep P&O algorithm is introduced.

4.2.2 MULTISTEP PERTURB AND OBSERVE MPPT ALGORITHM

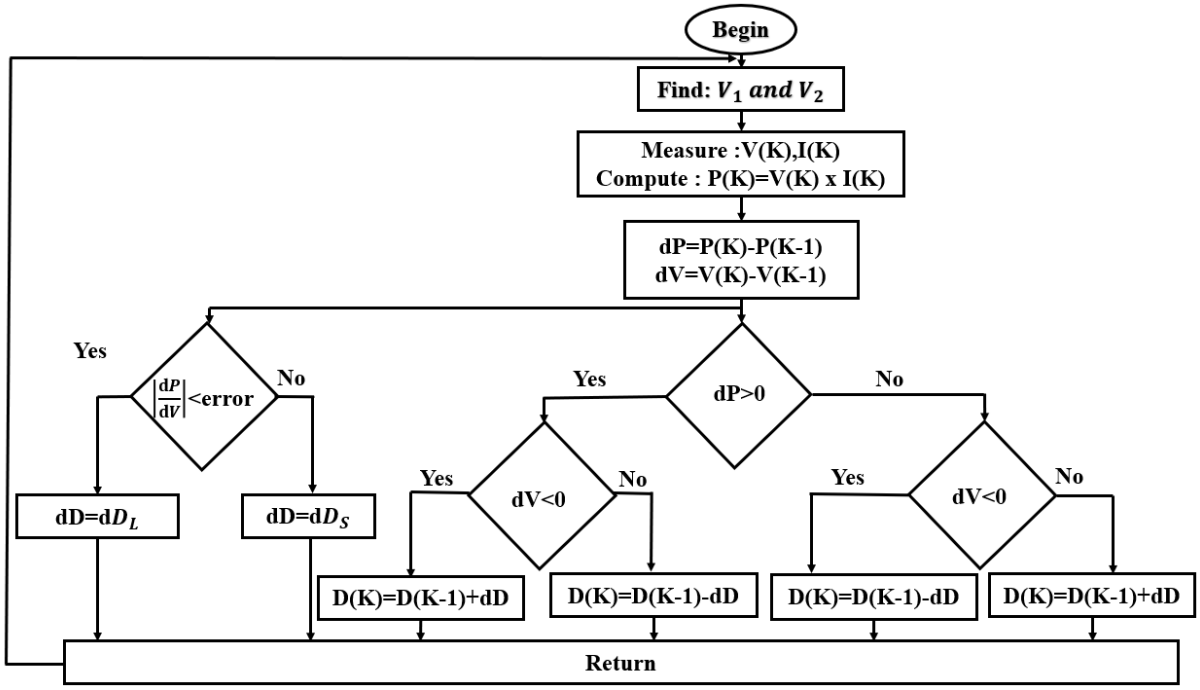

Figure 4.2: Flow chart of multistep P&O algorithm

Multistep P&O is the improved version of conventional P&O, which increases the tracking speed and reduces the oscillations by comparing change in voltage with an error, either a high step value or a small step value is employed to achieve MPP. Figure 4.2 shows the flow chart of multistep P&O algorithm. When the operating point is far from MPP, the algorithm creates a large step value(0.02) and when the operating point is close to MPP, the algorithm creates small step value(0.002).By taking the slop of the P-V curve. In order to eliminate the limitations of P&O and multistep P&O algorithm a new method is introduced called zero oscillation MPPT algorithm.

4.2.3 ZERO OSCILLATION MPPT ALGORITHM

The zero oscillation method acquires the MPP faster and better than the P&O method because it doesn't have drifting problems and works most efficiently in rapidly changing environmental conditions. Two voltage and current sensors are used in this method to measure the output voltage and current of the PV array. This method is considered to be the slope of the power voltage curve. Figure 4.3 shows the flow chart of zero oscillation algorithm.

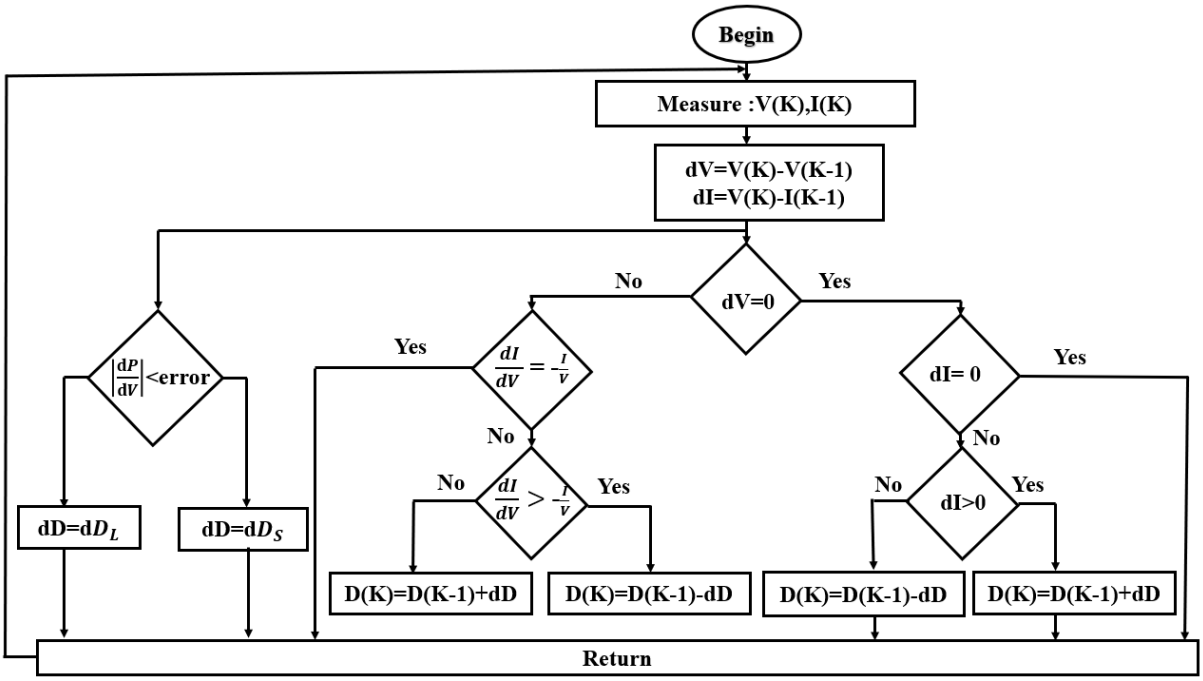

Figure 4.3: Flow chart of zero oscillation algorithm

This algorithm detects the slope of P-V curve. This algorithm uses instantaneous conductance $\frac{\mathrm{I}}{\mathrm{V}}$ and additive conductance $\frac{d_I}{d_V}$ for MPPT. The relation between the two conductance value is given by the equation 4.1

$$\frac{d_I}{d_V} = -\frac{\mathrm{I}}{\mathrm{V}} \tag{4.1}$$

$$\frac{d_I}{d_V} > -\frac{\mathrm{I}}{\mathrm{V}} \tag{4.2}$$

$$\frac{d_I}{d_V} < -\frac{\mathrm{I}}{\mathrm{V}} \tag{4.3}$$

Depending on the relationship between the two values, the operating point of PV panel in the P-V curve can be determined. Equation 4.1 indicates that the PV panel operates at MPP, equation 4.2 and 4.3 indicates that the operating point of the PV panel is on the left and right side of the P-V curve respectively.

4.3 SUMMARY

This chapter discusses different MPPT algorithms such as conventional P&O algorithm, multi-step P&O and zero oscillation algorithms , and their flow chart, advantages and disadvantages. These algorithms are employed in interleaved boost converter for the comparison and conclusion is depicted in the next chapter. The simulation model of the proposed system and the results are also included in chapter 5.

Chapter 5

SIMULATION MODEL AND RESULTS

5.1 OVERVIEW

This chapter deals with the design and simulation of proposed system with fixed DC source, PV source and integrated DC and PV source. The simulation and results of interleaved bidirectional converter, interleaved boost converter and voltage doubler are also included. These circuits are simulated in MATLAB/SIMULINK using the designed parameters and the simulation results are analysed.

5.2 SIMULATION PARAMETERS OF THE PROPOSED SYSTEM

Table 5.1: Simulation parameters of the proposed system.

SL.no	Parameter	Specification
1	Input Voltage(V_1)	60V
2	Switching Frequency(f_s)	30 KH_z
3	Power(P)	800W
4	Output Voltage(V_2)	240V

Table 5.1 shows the basic simulation parameters such as voltage, frequency, power and output voltages to design the converter parameters such as inductor, capacitor and resistor.

5.3 DESIGN EQUATIONS OF THE PROPOSED SYSTEM

A 800 W, 60/120 V, 30 KH_Z prototype is used to verify the proposed converter. The inductor, capacitor and resistor of the circuit are designed using the following equations:

- D_p denotes the duty cycle of the LVS.

$$D_P = 1 - \frac{V_1}{V_2} \tag{5.1}$$

- D_s denotes the duty cycle of the HVS.

$$D_S = D_p - \Delta D \tag{5.2}$$

- Inductor :

  The inductor ripple current is taken as 3% of the output current

$$L = \frac{V_1}{F_s \Delta I_L} D_p \tag{5.3}$$

- Capacitor at LVS :

  The voltage ripple is taken as 5% of the output voltage

$$C = \frac{I_D}{F_s \Delta V_0} D_p \tag{5.4}$$

- Capacitor at HVS :

  The Ripple voltage V_r is taken as 2%

$$C = \frac{t \times I}{V_r} \tag{5.5}$$

- Resistor :

$$R = \frac{V^2}{P} \tag{5.6}$$

5.4 DESIGN PARAMETERS OF THE PROPOSED SYSTEM

The designed parameters such as inductor, capacitor and resistor of the proposed system is shown in Table 5.2, which is calculated from the design equations mentioned above. L_1, L_2, C_1 and R_1 are the inductance, capacitance and resistance on the LVS. C_2, C_3 and R_2 are the capacitance and resistance on the HVS.

Table 5.2: Design parameters of the proposed system

SL.no	Parameter	Specification
1	Inductor(L_1, L_2)	1010.1 μH
2	Capacitor(C_1)	4.582 μF
3	Capacitor(C_2, C_3)	2.775 mF
4	Resistor(R_1)	18 Ω
5	Resistor(R_2)	72 Ω

Table 5.3 shows the PV specifications. Here we uses a PV panel with 2 parallel and 2 series strings and the output power of the panel is 800W

Table 5.3: PV specifications

SL.no	Parameter	Specification
1	Cells /Module(N_{cells})	60
2	Maximum power(W)	200 W
3	Open circuit voltage(V_{oc})	36 V
4	Short circuit current(I_{sc})	7.75 A
5	Voltage at maximum power point(V_{mp})	28.7 V
6	Current at maximum power point(I_{mp})	6.97 A
7	Temperature coefficient of V_{oc}	-0.126°C
8	Temperature coefficient of I_{sc}	0.055°C

5.5 SIMULATION MODEL AND RESULTS OF INTERLEAVED BIDIRECTIONAL CONVERTER CIRCUIT

Figure 5.1 shows the simulation model of interleaved bidirectional converter. It consist of four switches, inductor, capacitor and resistor. It consist of two modes of operation. One is boost mode of operation and the other is buck mode of operation. In boost mode of operation the

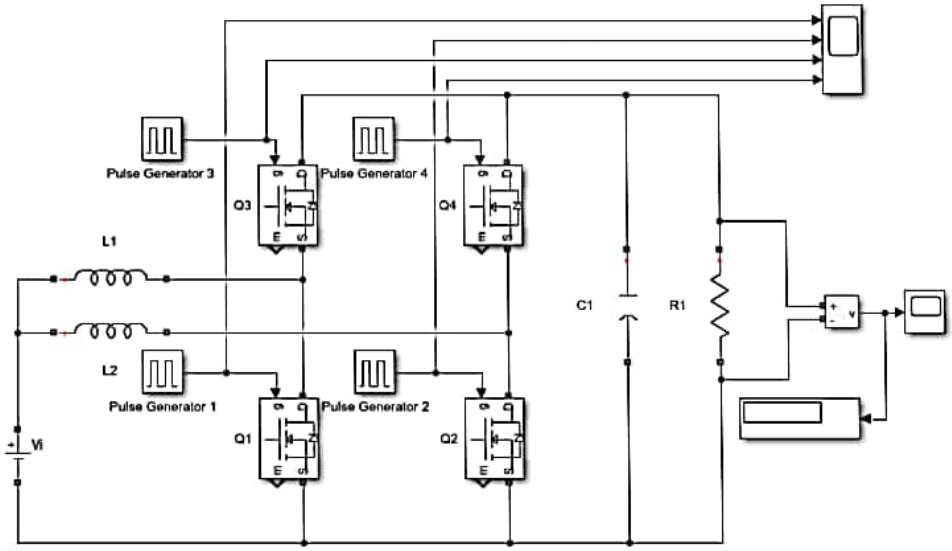

Figure 5.1: Simulation model of interleaved bidirectional converter circuit

voltage is boosted to voltage which is higher than the input voltage and in buck mode of operation the voltage is stepped down to a voltage which is less than the input voltage. Switching is used to make this device work in the boost and buck modes respectively. Switches Q_1 and Q_2 operates during the boost mode and Switches Q_3 and Q_4 operates during the buck mode of operation. When the power is turned on, the circuit is in boost mode for the first one second. For the next second, it will be working in buck mode.

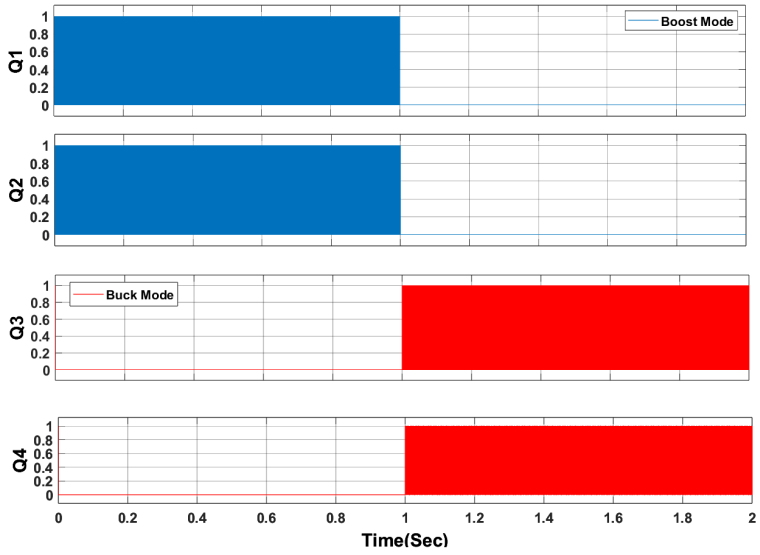

Figure 5.2: Switching pulses of interleaved bidirectional converter circuit

The switching pulses of an interleaved bidirectional converter are shown in Figure 5.2. It operates in boost mode for the first one second and switches to buck mode after one second.

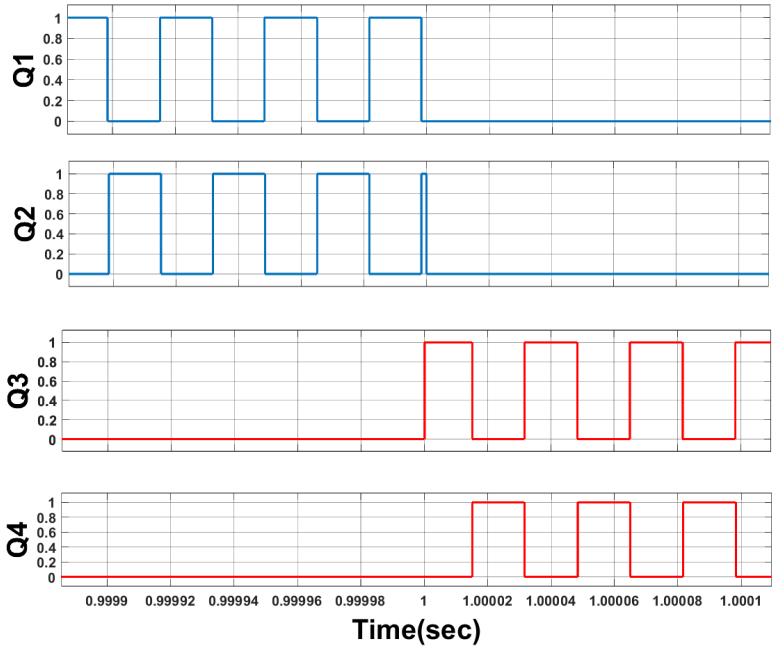

Figure 5.3: Enlarged switching pulses of interleaved bidirectional converter circuit

The enlarged switching pulses of interleaved bidirectional converter circuit with a duty ratio of 0.5 is shown in Figure 5.3. In boost mode switches Q_1 and Q_2 are triggered for first one second. For the next one second it will be in buck modes, during this mode switches Q_3 and Q_4 are triggered.

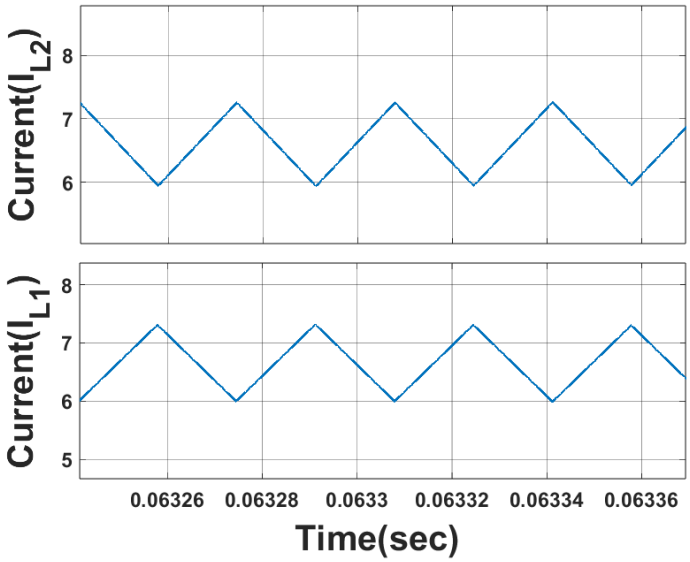

Figure 5.4: Inductor current of interleaved bidirectional converter circuit in boost mode

The inductor current in an interleaved bidirectional converter in boost mode is shown in Figure 5.4. Inductor currents I_{L1} and I_{L2} are increasing during boost mode with 180 °phase shift. The

input current is the average of these two inductor current, so ripple will be less as compared to conventional boost converter.

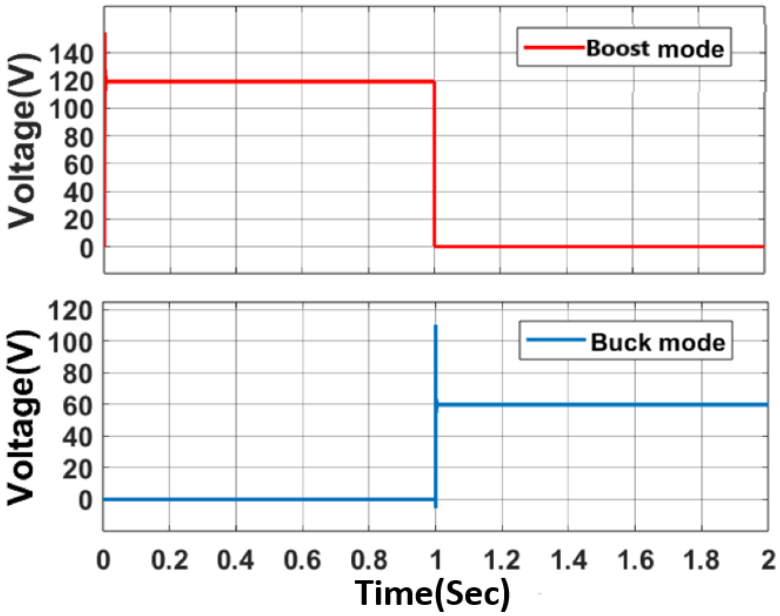

Figure 5.5: Output voltage of interleaved bidirectional converter

The output voltage of interleaved bidirectional converter is shown in Figure 5.5. The red line indicates the boost mode of operation and the blue line indicates the buck mode of operation of interleaved bidirectional converter. For the first one second, the switching pulse is in boost mode, and the voltage is boosted to 120 volts. After one second, as it is in buck mode, the voltage is stepped down to 60 volts.

5.6 SIMULATION MODEL AND RESULTS OF INTERLEAVED BOOST CONVERTER CIRCUIT

The simulation model of interleaved boost converter is shown in Figure 5.6. It consist of a inductor, capacitor and resistor. Here for the boost operation only the switches Q_1 and Q_2 are triggered. Here only the boost mode of operation is considered to obtain high gain.

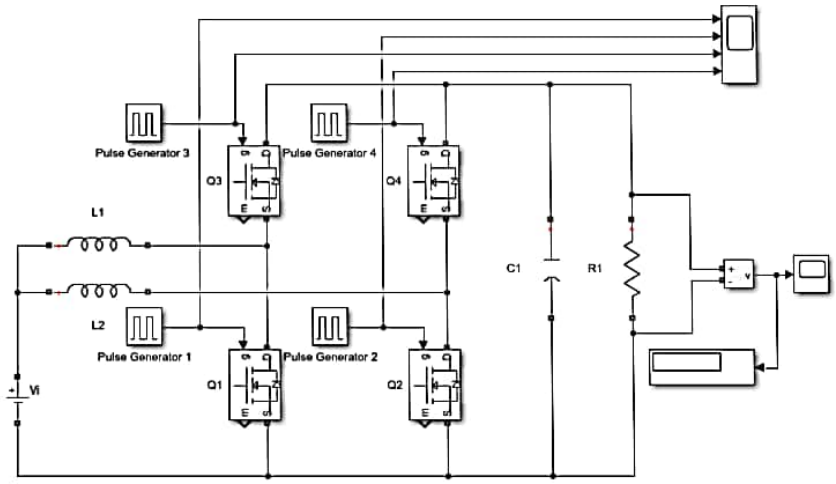

Figure 5.6: Simulation model of interleaved boost converter circuit

The duty ratio of the interleaved boost converter with P&O algorithm is shown in Figure 5.7. The duty ratio increases step by step from 0.1 to 0.52 upto a time of 0.42 sec. After 0.42 sec duty ratio will remain stable with oscillations. Conventional P&O will take some time to reach desired duty ratio.

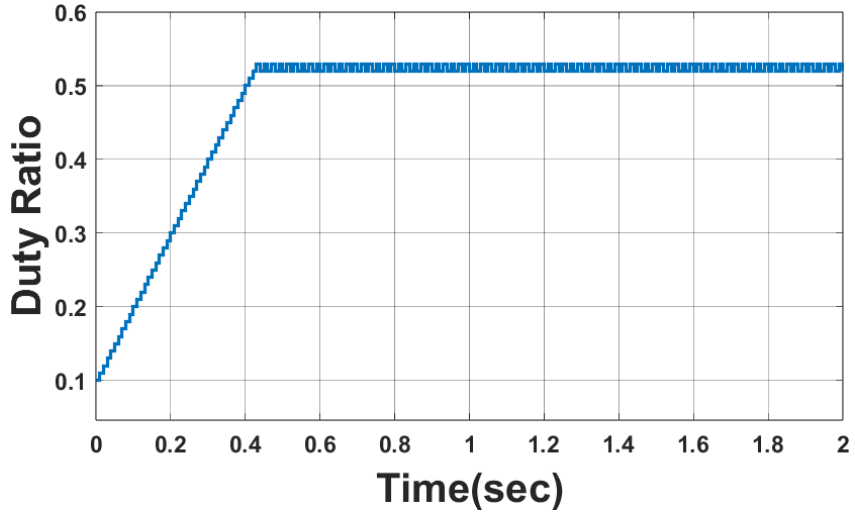

Figure 5.7: Duty ratio of interleaved boost converter with P&O algorithm

The output voltage of the interleaved boost converter with P&O algorithm is shown in Figure 5.8. Graph shows that output voltage reaches its desired value after 0.42 second. The average voltage and percentage ripple of output is calculated from the graph as 119V and 1.17 percentage respectively. To overcome this multistep P&O algorithm is introduced.

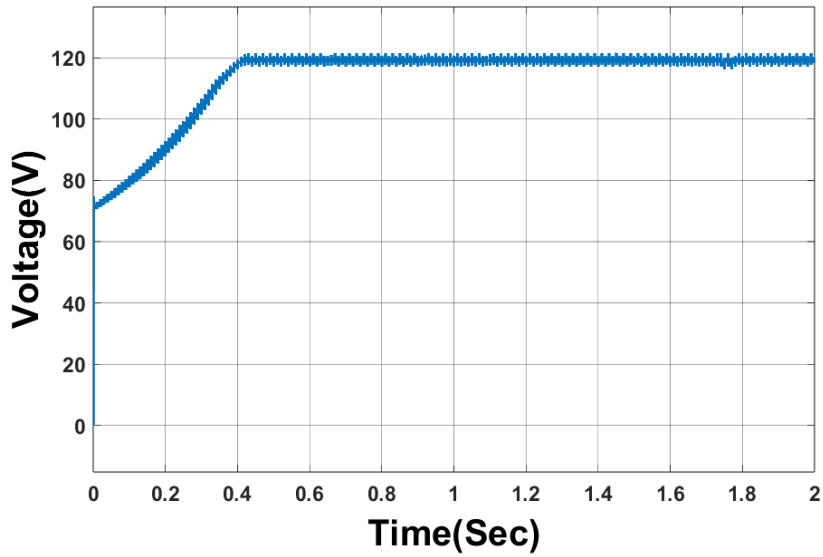

Figure 5.8: Output voltage of interleaved boost converter with P&O algorithm

The duty ratio of interleaved boost converter with multistep P&O algorithm is shown in Figure 5.9. Duty ratio reaches its desired value at 0.2 sec, multistep P&O algorithm reaches desired value much faster than conventional P&O algorithm with less oscillation.

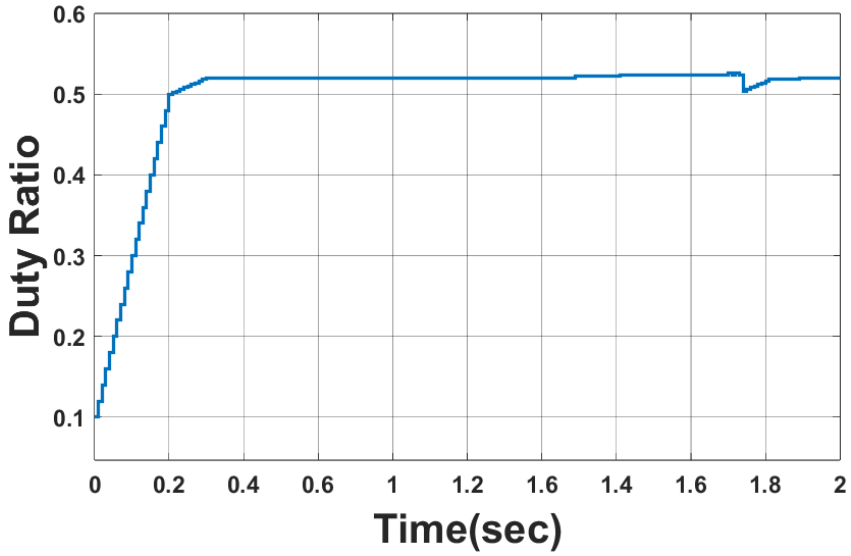

Figure 5.9: Duty ratio of interleaved boost converter with multistep P&O algorithm

The output voltage of the interleaved boost converter with multi-step P&O algorithm is shown in Figure 5.10. The output voltage reaches the desired value after 0.2 sec, with a ripple percentage of 1.005%. The average output voltage is 119.2V.

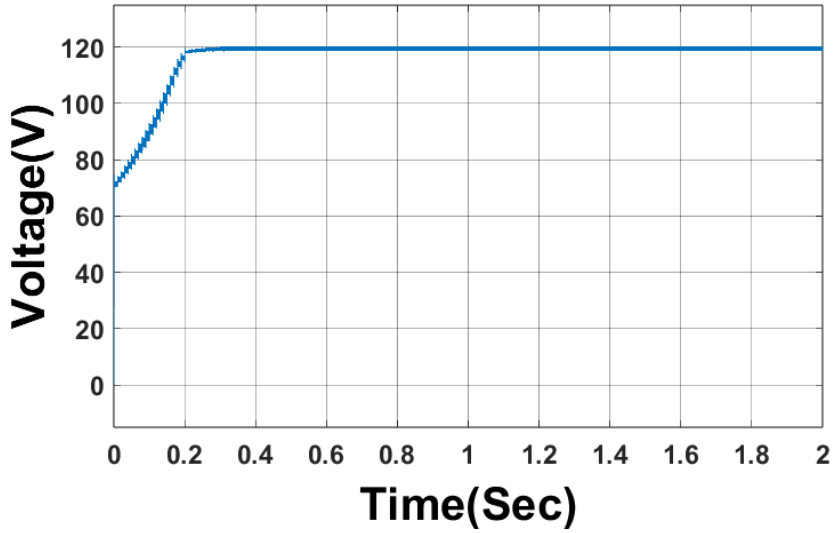

Figure 5.10: Output voltage of interleaved boost converter with multistep P&O algorithm

The duty ratio of interleaved boost converter with zero oscillation algorithm is shown in Figure 5.11. This method acquires steady state much faster than aforementioned MPPT algorithms. Zero oscillation algorithm attains the desired duty ratio at 0.034 seconds.

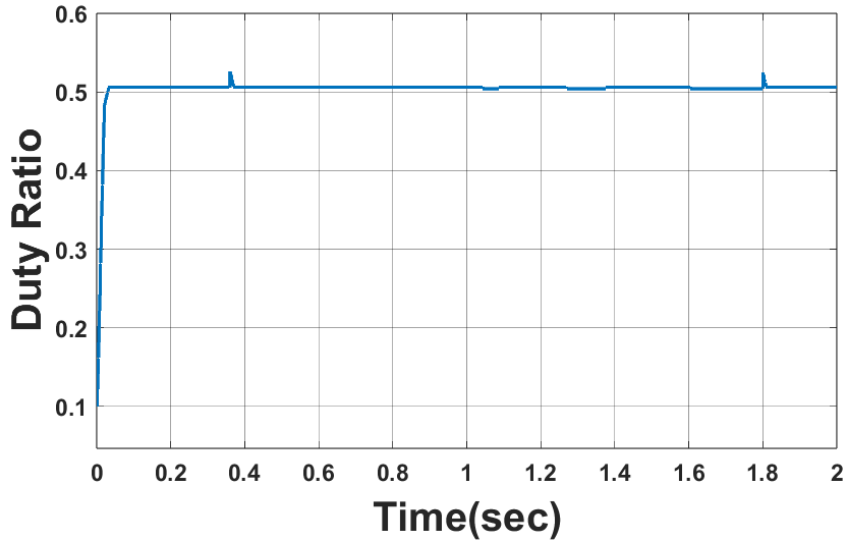

Figure 5.11: Duty ratio of interleaved boost converter with zero oscillation algorithm

The output voltage of the interleaved boost converter with zero oscillation MPPT algorithm is shown in Figure 5.12. The output voltage has a ripple percentage of 0.8%, which is less than the ripples produced in conventional P&O and multistep P&O algorithms. Here the average output voltage 119.5V.

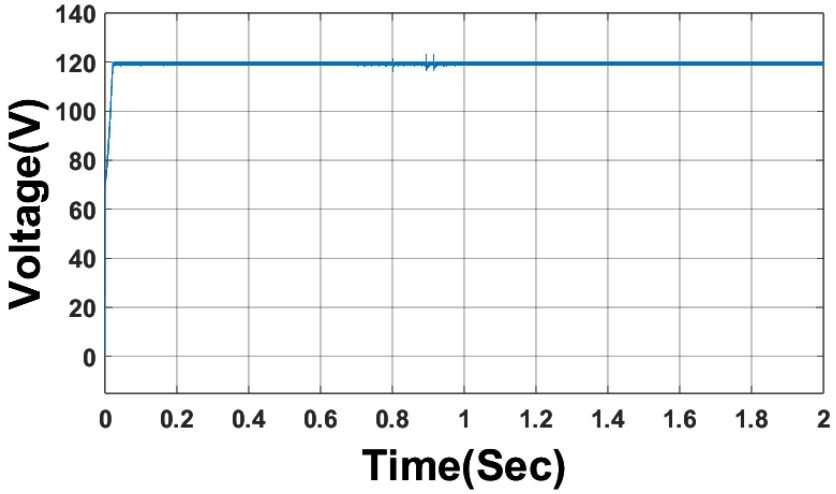

Figure 5.12: Output voltage of interleaved boost converter with zero oscillation algorithm

Table 5.4: Comparison of three MPPT method

Time taken to reach MPPT(Sec)	MPPT methods	Average Voltage(V)	Ripple Percentage(%)
0.42	P&O	119.2	1.17
0.2	Multistep P&O	119.3	1.005
0.034	Zero Oscillation	119.35	0.8

Table 5.4 depicts the comparison of three MPPT algorithms. This comparison led to the conclusion that the zero oscillation algorithm is better than other P&O and multistep P&O algorithm as the ripple of the output voltage is reduced and the time taken to reach MPP is much faster. Hence for further simulation only Zero oscillation MPPT algorithm is used with solar PV panel.

5.7 SIMULATION MODEL OF VOLTAGE DOUBLER CIRCUIT

The simulation model of voltage doubler circuit is shown in figure 5.13. It consist of capacitor, resistor, and switches. The voltage doubler doubles the output voltage. At the first stage, when S1 is ON, the diode D_1 is forward biased, which allows the current to flow through it. This

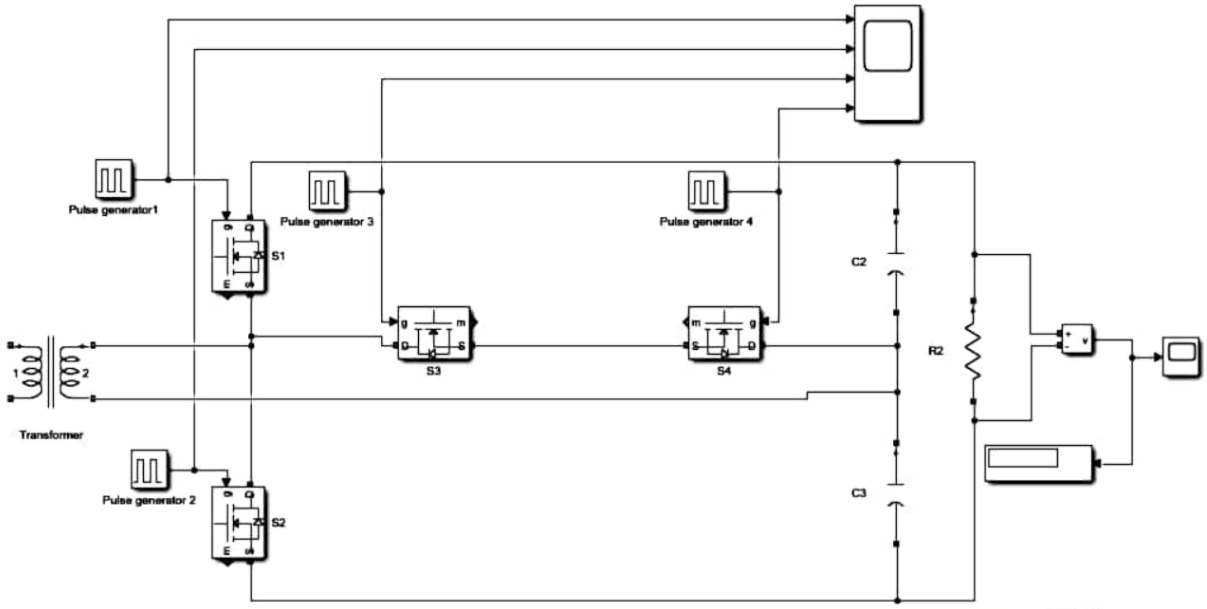

Figure 5.13: Simulation model of voltage doubler circuit

current passes through the capacitor C_2 and charges it to the peak value of the input voltage. At that time, S_2 is OFF, and the diode of D_2 is reverse biased. So it does not allow the current to flow through it, thus the capacitor C_3 is uncharged. When switch S_1 is OFF and S_2 is in ON condition, the reverse operation will take place. The capacitor C_3 charges and C_2 becomes uncharged. C_3 also charges to the peak value of the input voltage. So the total output voltage (V_2) will be the sum of the voltages across two capacitors. Switches S_3 and S_4 indicates the bidirectional operation.

5.8 SIMULATION MODEL OF THE SYSTEM

The simulation model of the whole system is shown in Figure 5.14, which consist of DC-DC converter, PPS control, MPPT control and switching case. DC-DC converter consists of an inductor(L), capacitor(C), resistor(R), and eight switches. Q_1, Q_2, Q_3, Q_4 in LVS side and S_1, S_2, S_3, S_4 in HVS. D_P denotes the duty cycle of LVS side. The drive signal of Q_1 lags behind the drive signal of Q_2 by 180°. Meanwhile, the drive signals of Q_1, and Q_2 are complementary with those of Q_3 and Q_4. D_S denoted the duty cycle of the HVS side. The drive signal of S_3 also lags behind the drive signal of S_4. Meanwhile, the drive signals of S_3 and S_4 are complementary with those of S_1 and S_2 by 180°.

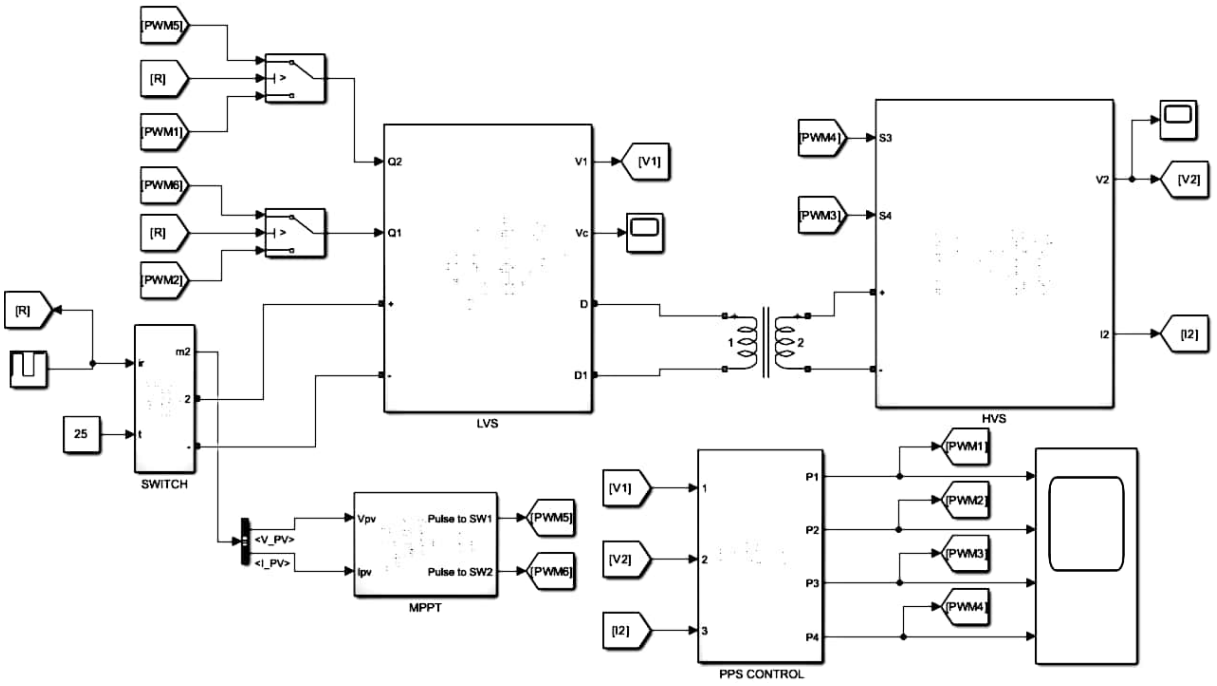

Figure 5.14: Simulation model of the system

60V is given as the input which is gone for interleaved boost operation in LVS. Thus the voltage is boosted to an average voltage of 120V. This boosted voltage is passed through an isolation transformer. After that it will undergo for voltage doubling operation where the voltage get doubled to an average of 240V. In PPS control, the input is the input voltage from the LVS side and the output pulses from PWM are given to the switches Q_1, Q_2 in LVS side and S_1, S_2, S_3, S_4 in HVS. In MPPT control, the output pulses from PWM are given to the switches Q_1, Q_2.

5.9 SIMULATION RESULTS OF THE PROPOSED SYSTEM

Based on the input source applied to the proposed system there are three cases of operation. They are the system with:

- Fixed DC source
- PV source
- PV source and fixed DC source

5.9.1 WITH FIXED DC SOURCE

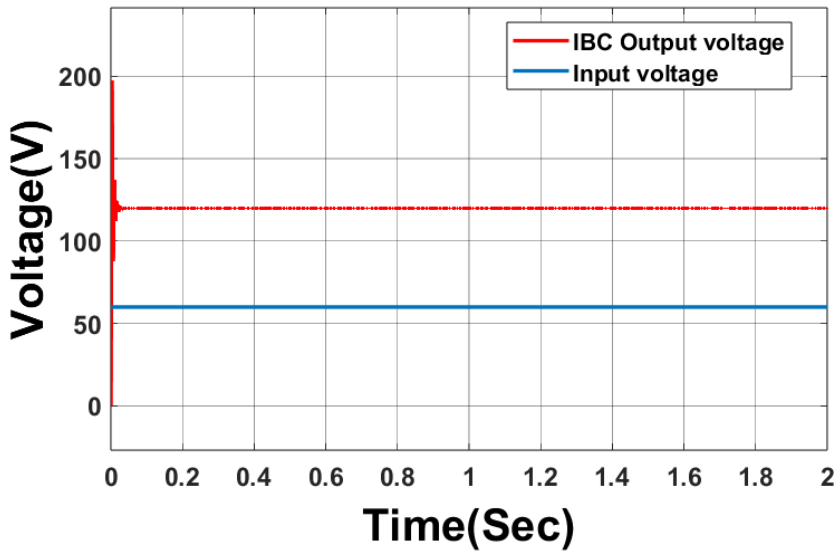

Figure 5.15: Input and output voltage of interleaved boost converter with DC source

The input voltage and the output voltage (V_c) of the interleaved boost converter in the proposed system with fixed DC source is shown in Figure 5.15. The input voltage is 60V which is a constant throughout the operation.The output voltage of the interleaved boost converter, is a boosted voltage which is an average of 119V. The interleaved circuit eliminates the ripples in the output voltage of LVS.

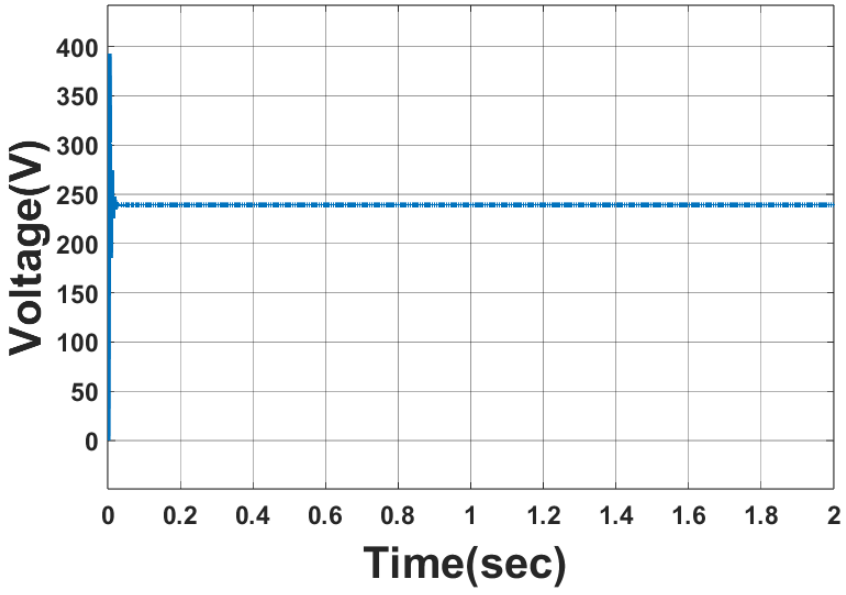

Figure 5.16: Output voltage of the proposed system with DC source

The output voltage of the proposed system with a DC source is shown in Figure 5.16. The average voltage and percentage ripple is calculated from the output voltage waveform are 238V and 0.8 percentage respectively,leads to the conclusion that proposed system provides desired constant DC supply with less ripples.

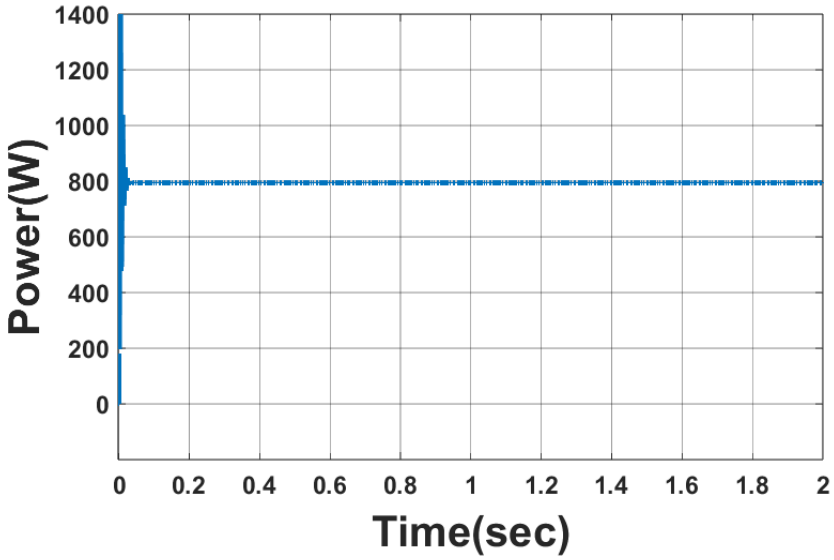

Figure 5.17: Output power of the proposed system with DC source

The output power of the proposed system with DC source is shown in Figure 5.17. The average power and efficiency estimated from the output power waveform are 790W and 98.75%, respectively, which leads to the conclusion that the proposed system provides better efficiency at fixed DC input voltage.

5.9.2 WITH PV SOURCE

The input and output voltage of the interleaved boost converter in the proposed system with PV source is shown in Figure 5.18. The input voltage given to the converter is 60V, which is boosted to an average of 119V. The input and output voltage of the interleaved boost converter is indicated by the blue line and red line respectively.

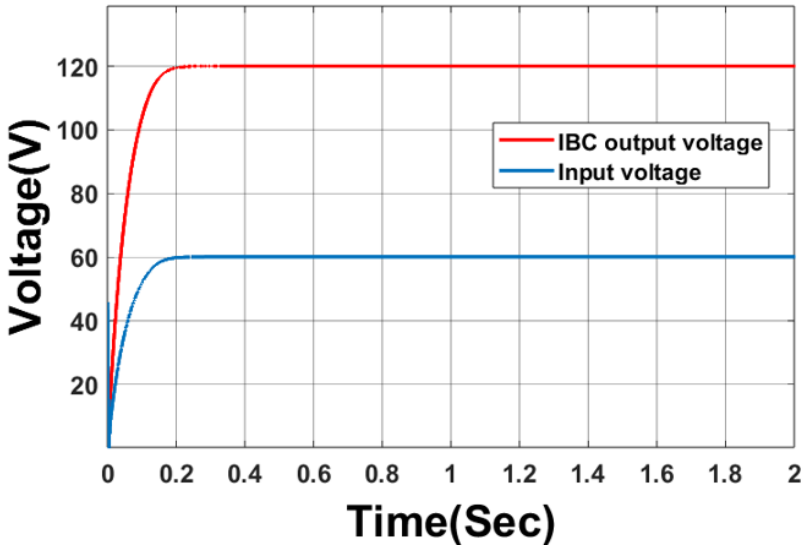

Figure 5.18: Input and output voltage of the interleaved boost converter with PV source

The output voltage of the proposed system with PV source is shown in Figure 5.19. The output voltage is double the output voltage produced at interleaved boost converter. The average voltage and ripple factor obtained from the voltage waveform is 238.5V and 0.88%.

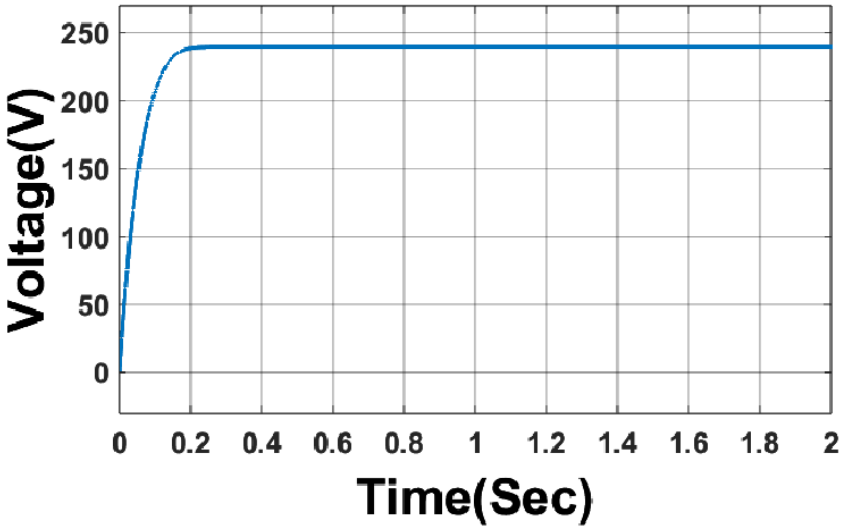

Figure 5.19: Output voltage of the proposed system with PV source

The output power of the proposed system with a PV source is shown in Figure 5.20. The output power waveform provided an average power and efficiency of 792W and 99% respectively, which led to the conclusion that the system using a PV source has a better efficiency.

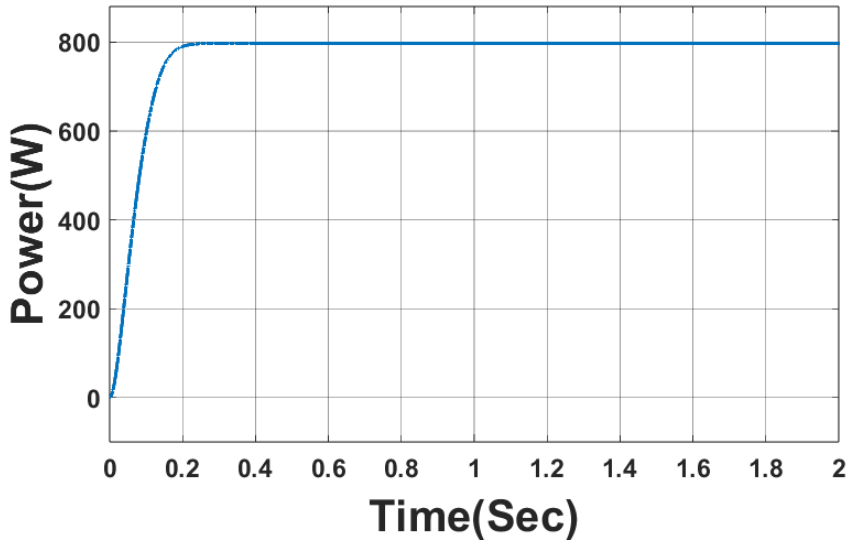

Figure 5.20: Output power of the proposed system with PV source

5.9.3 WITH PV AND FIXED DC SOURCE

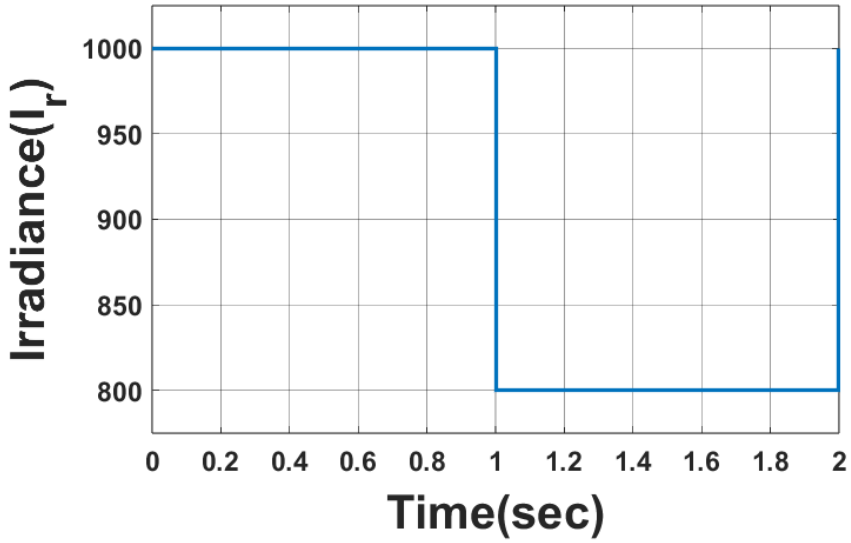

Figure 5.21: Irradiance value of the proposed system with PV and DC source

The irradiance value of the proposed system is shown in Figure 5.21. Standard value of irradiance and temperature is used for the analysis. A reference value is set for irradiance for switching. Above the reference value, the system works with a PV source, and below the reference value, the system works with a DC source.

The duty ratio of the proposed system when changing from PV array to dc source is shown in Figure 5.22. Here from 0-1 sec the solar will be working with PV source. After 1 sec the DC source will supply power to the system.

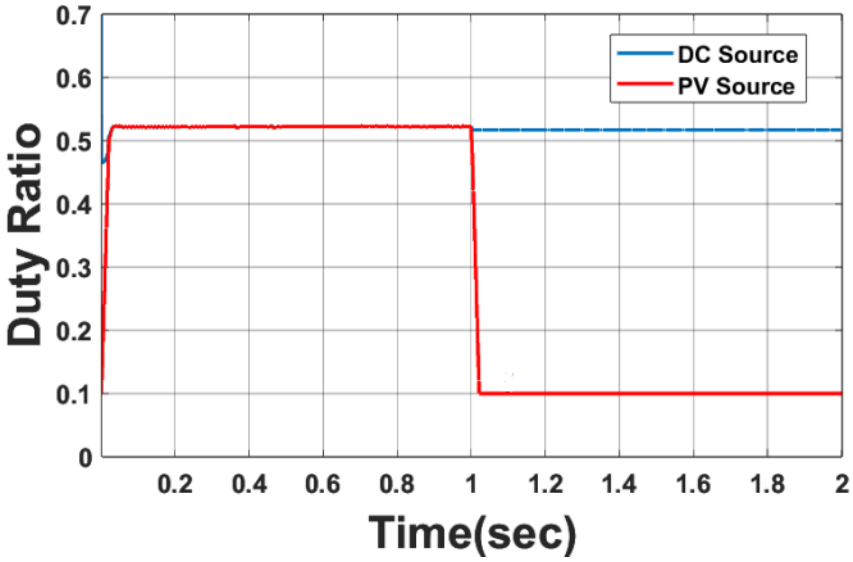

Figure 5.22: Duty Ratio of interleaved boost converter with DC and PV source

The output voltage of the interleaved boost converter when changing from PV source to DC source is shown in Figure 5.23. There is a slight variation during the switching of PV to DC source at 1 sec. The average output voltage of the interleaved boost converter is 118V.

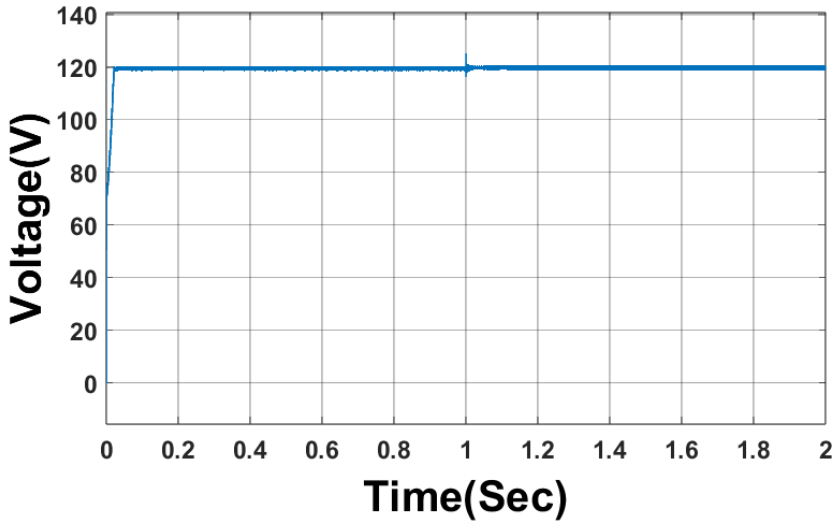

Figure 5.23: Output voltage of the interleaved boost converter with DC and PV source

The output voltage of the proposed system with DC and PV sources is shown in Figure 5.24. For the first one second, the system will be working under PV source, and after that, it works under DC source. A slight variation occurs at 1 sec due to the changing the system from PV source to DC source. The average voltage and ripple obtained from waveform of the system is 239V and 0.8 % respectively.

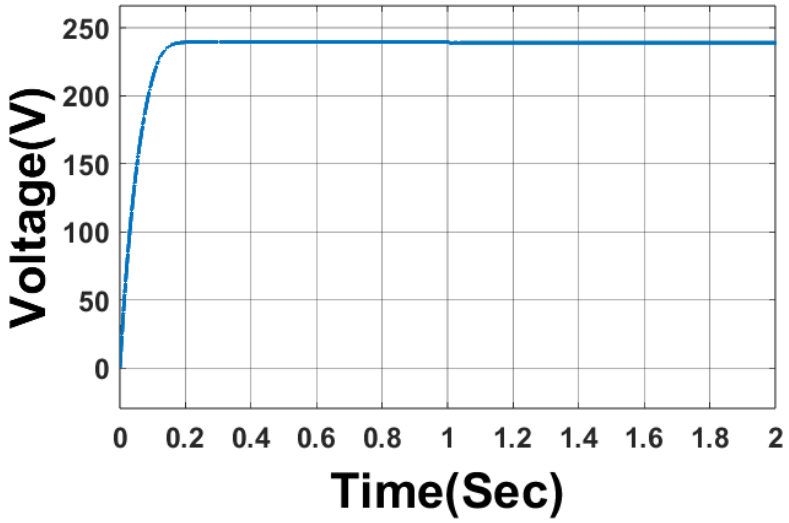

Figure 5.24: Output voltage of the proposed system with DC and PV source

The output power of the proposed system using DC and PV sources is shown in Figure 5.25. The system will operate on a PV source for the first second, and then switch to a DC source. When changing from a PV source to a DC source, there is variation occurs after 1 second in the output. Waveform analysis shows that the system's average output power is 794W, and its average efficiency is 99.2%.

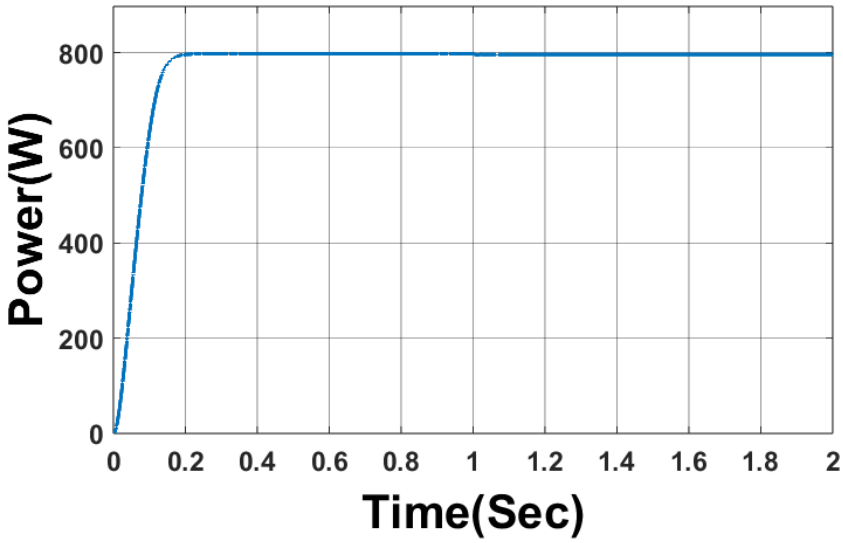

Figure 5.25: Output power of the proposed system with DC and PV source

5.10 SUMMARY

Interleaved bidirectional converter, proposed system with interleaved boost converter and voltage doubler circuits are simulated using the design parameters. From the different MPPT methods such as P&O, multistep P&O and zero oscillation algorithm used in interleaved boost converter, summarises that zero oscillation algorithm is much better than other aforementioned algorithms. Therefore zero oscillation MPPT algorithm is used for the proposed system to extract maximum power point. The proposed system works with DC source, PV source and integrated DC and PV source as the input to the interleaved boost converter. Proposed system with DC source provides an average output voltage, power and efficiency of 238V, 780W and 98.75% respectively.The proposed system with PV source provides an average output voltage, power and efficiency of 238.5V, 792W and 99% respectively. When both DC and PV sources are used as the input to the proposed system, the input source changes from DC to PV source when the irradiance value is less than the reference value. 239V, 794W and 99.2% are the average output voltage, power and efficiency of the proposed system with both DC and PV as the input source to the proposed system.

Chapter 6

CONCLUSION

6.1 CONCLUSIONS

A high-gain bidirectional converter with a PPS control strategy is used for output voltage regulation. An interleaved bidirectional converter in the LVS reduces the output voltage and current ripple, and a voltage doubler in the HVS is used to obtain high voltage gain without using a transformer with a high turn ratio. The proposed system works with two input sources, such as a fixed DC source and a PV source. The proposed system provides better efficiency at a fixed DC input voltage with a ripple of 0.8%. In order to develop a sustainable way to charge EVs, the PV panel is used as the input to the proposed system. The maximum solar power is obtained by using MPPT algorithms, and here three MPPT algorithms, such as P&O, multistep P&O, and zero oscillation algorithms, are used to harvest the maximum power point from the proposed system. From the comparison of three MPPT methods, it is concluded that the zero oscillation method is better for achieving maximum power at a lower time. The efficiency of the proposed system increases as it reaches its maximum power point. As solar energy is an unreliable source of energy, the proposed system automatically switches from a PV to a DC source depending on solar irradiance. The efficiency of the proposed system with a DC source, a PV source, and both PV and DC sources is 98.75%, 99%, and 99.2%, respectively. Thus, the system becomes more cost-effective and reliable.

6.2 SCOPE FOR FUTURE WORK

In this work, a high-voltage-gain bidirectional DC-DC converter is developed. In future work, DC and PV sources can be operated at the same time so that it gets power from both sources. Implementation of advanced MPPT methods can also be used as a modification to future work.

REFERENCES

[1] A. Chub, D. Vinnikov, R. Kosenko, E. Liivik, and I. Galkin, "Bidirectional dc–dc converter for modular residential battery energy storage systems," *IEEE Transactions on Industrial Electronics*, vol. 67, no. 3, pp. 1944–1955, 2019.

[2] T. Dragičević, X. Lu, J. C. Vasquez, and J. M. Guerrero, "Dc microgrids—part ii: A review of power architectures, applications, and standardization issues," *IEEE transactions on power electronics*, vol. 31, no. 5, pp. 3528–3549, 2015.

[3] H.-J. Chiu and L.-W. Lin, "A bidirectional dc–dc converter for fuel cell electric vehicle driving system," *IEEE Transactions on Power Electronics*, vol. 21, no. 4, pp. 950–958, 2006.

[4] B. Zhao, Q. Yu, and W. Sun, "Extended-phase-shift control of isolated bidirectional dc–dc converter for power distribution in microgrid," *IEEE Transactions on power electronics*, vol. 27, no. 11, pp. 4667–4680, 2011.

[5] X. Shi, J. Jiang, and X. Guo, "An efficiency-optimized isolated bidirectional dc-dc converter with extended power range for energy storage systems in microgrids," *Energies*, vol. 6, no. 1, pp. 27–44, 2012.

[6] H. Qian, J. Zhang, J.-S. Lai, and W. Yu, "A high-efficiency grid-tie battery energy storage system," *IEEE transactions on power electronics*, vol. 26, no. 3, pp. 886–896, 2010.

[7] P. Xuewei and A. K. Rathore, "Novel bidirectional snubberless naturally commutated soft-switching current-fed full-bridge isolated dc/dc converter for fuel cell vehicles," *IEEE Transactions on Industrial Electronics*, vol. 61, no. 5, pp. 2307–2315, 2013.

[8] T. Mishima, H. Mizutani, and M. Nakaoka, "A sensitivity-improved pfm llc resonant full-bridge dc–dc converter with lc antiresonant circuitry," *IEEE Transactions on power electronics*, vol. 32, no. 1, pp. 310–324, 2016.

[9] K. S. Chitanya and P. Raghavendran, "Isolated bidirectional full-bridge dc–dc converter with a flyback snubber," *International Journal of Soft Computing and Engineering (IJSCE)*, vol. 3, no. 2, 2013.

[10] R. W. De Doncker, D. M. Divan, and M. H. Kheraluwala, "A three-phase soft-switched high-power-density dc/dc converter for high-power applications," *IEEE transactions on industry applications*, vol. 27, no. 1, pp. 63–73, 1991.

[11] B. Zhao, Q. Song, J. Li, and W. Liu, "A modular multilevel dc-link front-to-front dc solid-state transformer based on high-frequency dual active phase shift for hvdc grid integration," *IEEE Transactions on Industrial Electronics*, vol. 64, no. 11, pp. 8919–8927, 2016.

[12] N. Yousefpoor, B. Parkhideh, A. Azidehak, S. Kim, and S. Bhattacharya, "Control of high-frequency isolated modular converter," *IEEE Transactions on Industry Applications*, vol. 51, no. 6, pp. 4634–4641, 2015.

[13] F. An, W. Song, B. Yu, and K. Yang, "Model predictive control with power self-balancing of the output parallel dab dc–dc converters in power electronic traction transformer," *IEEE Journal of Emerging and Selected Topics in Power Electronics*, vol. 6, no. 4, pp. 1806–1818, 2018.

[14] C. Mi, H. Bai, C. Wang, and S. Gargies, "Operation, design and control of dual h-bridge-based isolated bidirectional dc–dc converter," *IET Power Electronics*, vol. 1, no. 4, pp. 507–517, 2008.

[15] D. Sha, Y. Xu, J. Zhang, and Y. Yan, "Current-fed hybrid dual active bridge dc–dc converter for a fuel cell power conditioning system with reduced input current ripple," *IEEE Transactions on Industrial Electronics*, vol. 64, no. 8, pp. 6628–6638, 2017.

[16] H. Seok, B. Han, B.-H. Kwon, and M. Kim, "High step-up resonant dc–dc converter with ripple-free input current for renewable energy systems," *IEEE Transactions on Industrial Electronics*, vol. 65, no. 11, pp. 8543–8552, 2018.

[17] S. Bal, D. B. Yelaverthi, A. K. Rathore, and D. Srinivasan, "Improved modulation strategy using dual phase shift modulation for active commutated current-fed dual active bridge," *IEEE Transactions on Power Electronics*, vol. 33, no. 9, pp. 7359–7375, 2017.

[18] Z. Ding, C. Yang, Z. Zhang, C. Wang, and S. Xie, "A novel soft-switching multiport bidirectional dc–dc converter for hybrid energy storage system," *IEEE transactions on power electronics*, vol. 29, no. 4, pp. 1595–1609, 2013.

[19] L.-S. Yang and T.-J. Liang, "Analysis and implementation of a novel bidirectional dc–dc converter," *IEEE transactions on industrial electronics*, vol. 59, no. 1, pp. 422–434, 2011.

[20] Y.-P. Hsieh, J.-F. Chen, L.-S. Yang, C.-Y. Wu, and W.-S. Liu, "High-conversion-ratio bidirectional dc–dc converter with coupled inductor," *IEEE Transactions on Industrial Electronics*, vol. 61, no. 1, pp. 210–222, 2013.

[21] R.-Y. Duan and J.-D. Lee, "High-efficiency bidirectional dc-dc converter with coupled inductor," *IET Power Electronics*, vol. 5, no. 1, pp. 115–123, 2012.

[22] H. Moradisizkoohi, N. Elsayad, and O. A. Mohammed, "Experimental demonstration of a modular, quasi-resonant bidirectional dc–dc converter using gan switches for electric vehicles," *IEEE Transactions on Industry Applications*, vol. 55, no. 6, pp. 7787–7803, 2019.

[23] H. Bahrami, S. Farhangi, H. Iman-Eini, and E. Adib, "A new interleaved coupled-inductor nonisolated soft-switching bidirectional dc–dc converter with high voltage gain ratio," *IEEE Transactions on industrial electronics*, vol. 65, no. 7, pp. 5529–5538, 2017.

[24] M. Shreelakshmi, M. Das, and V. Agarwal, "Design and development of a novel high voltage gain, high-efficiency bidirectional dc–dc converter for storage interface," *IEEE transactions on industrial electronics*, vol. 66, no. 6, pp. 4490–4501, 2018.

[25] H. Yu, X. Xiang, H. Wu, G. Liu, W. Li, and X. He, "Performance comparison of phase-shift (ps) and pwm plus phase-shift (pps) control schemes for bidirectional dc-dc converters," in *2012 IEEE International Symposium on Industrial Electronics*. IEEE, 2012, pp. 447–452.

[26] Y. Shi, R. Li, Y. Xue, and H. Li, "Optimized operation of current-fed dual active bridge dc–dc converter for pv applications," *IEEE Transactions on Industrial Electronics*, vol. 62, no. 11, pp. 6986–6995, 2015.

[27] D. Sha, X. Wang, and D. Chen, "High-efficiency current-fed dual active bridge dc–dc converter with zvs achievement throughout full range of load using optimized switching patterns," *IEEE Transactions on Power Electronics*, vol. 33, no. 2, pp. 1347–1357, 2017.

[28] A. Tong, L. Hang, G. Li, X. Jiang, and S. Gao, "Modeling and analysis of a dual-active-bridge-isolated bidirectional dc/dc converter to minimize rms current with whole operating range," *IEEE Transactions on Power Electronics*, vol. 33, no. 6, pp. 5302–5316, 2017.

[29] W. Song, N. Hou, and M. Wu, "Virtual direct power control scheme of dual active bridge dc–dc converters for fast dynamic response," *IEEE Transactions on Power Electronics*, vol. 33, no. 2, pp. 1750–1759, 2017.

[30] N. Hou, W. Song, Y. Li, Y. Zhu, and Y. Zhu, "A comprehensive optimization control of dual-active-bridge dc–dc converters based on unified-phase-shift and power-balancing scheme," *IEEE Transactions on Power Electronics*, vol. 34, no. 1, pp. 826–839, 2018.

[31] J. Zeng, Z. Yan, J. Liu, and Z. Huang, "A high voltage-gain bidirectional dc–dc converter with full-range zvs using decoupling control strategy," *IEEE Journal of Emerging and Selected Topics in Power Electronics*, vol. 8, no. 3, pp. 2775–2784, 2019.

[32] S. Motahhir, A. El Hammoumi, and A. El Ghzizal, "The most used mppt algorithms: Review and the suitable low-cost embedded board for each algorithm," *Journal of cleaner production*, vol. 246, p. 118983, 2020.

[33] J. Udavalakshmi and M. S. Sheik, "Comparative study of perturb & observe and look-up table maximum power point tracking techniques using matlabisimulink," in *2018 international conference on current trends towards converging technologies (ICCTCT)*. IEEE, 2018, pp. 1–5.

[34] S. S. Mohammed, D. Devaraj, and T. I. Ahamed, "Maximum power point tracking system for stand alone solar pv power system using adaptive neuro-fuzzy inference system," in *2016 biennial international conference on power and energy systems: towards sustainable energy (PESTSE)*. IEEE, 2016, pp. 1–4.

[35] S. Sheik Mohammed and D. Devaraj, "Interleaved boost converter with perturb and observe maximum power point tracking algorithm for photovoltaic system," in *International Conference on Substantial Environmental Engineering and Renewable Energy*, 2015.

[36] E. Sarika, J. Jacob, M. S. Sheik, and S. Paul, "Performance analysis of solar photovoltaic system with fuzzy based variable step size mppt algorithm using matlab/simulink," in *2018 International Conference on Circuits and Systems in Digital Enterprise Technology (ICCSDET)*. IEEE, 2018, pp. 1–7.

[37] R. John, S. S. Mohammed, and R. Zachariah, "Variable step size perturb and observe mppt algorithm for standalone solar photovoltaic system," in *2017 IEEE International Conference on Intelligent Techniques in Control, Optimization and Signal Processing (INCOS)*. IEEE, 2017, pp. 1–6.

[38] A. Arancibia and K. Strunz, "Modeling of an electric vehicle charging station for fast dc charging," in *2012 IEEE International Electric Vehicle Conference*. IEEE, 2012, pp. 1–6.

[39] G. Naveen, T. H.-T. Yip, and Y. Xie, "Modeling and protection of electric vehicle charging station," in *2014 6th IEEE power india international conference (PIICON)*. IEEE, 2014, pp. 1–6.

[40] L. Kunjuramakurup, S. M. Sulthan, M. S. Ponparakkal, V. Raj, and M. Sathyajith, "A high-power solar pv-fed tiso dc-dc converter for electric vehicle charging applications," *Energies*, vol. 16, no. 5, p. 2186, 2023.